Report 1311

Copy 24

(2)

AD A043589

NANOOSE RANGE CURRENT CHARACTERISTICS AT 274m DEPTH

Research & Engineering Department

May 1977

Approved for public release; distribution unlimited

NAVAL TORPEDO STATION
Keyport, Washington 98345

DEPARTMENT OF THE NAVY
NAVAL TORPEDO STATION
KEYPORT, WASHINGTON 98345

JOHN G. FLETCHER
CAPT, USN
COMMANDING OFFICER

R. D. MELIM
CDR, USN
EXECUTIVE OFFICER

E. H. LESINSKI
TECHNICAL DIRECTOR

ADMINISTRATIVE STATEMENT

NAVTORPSTA Report 1311, *Nanoose Range Current Characteristics at 274m Depth*

By Robert A. Helton and James R. Holbrook

Prepared under internal range improvement funds

Released by: R. L. Marimon

R. L. MARIMON, Head
Research & Engineering Department
May 1977

UNCLASSIFIED

SECURITY CLASSIFICATION OF THIS PAGE (When Data Entered)

REPORT DOCUMENTATION PAGE

READ INSTRUCTIONS BEFORE COMPLETING FORM

1. REPORT NUMBER: 1311

2. GOVT ACCESSION NO.

3. RECIPIENT'S CATALOG NUMBER

4. TITLE (and Subtitle): (6) NANOOSE RANGE CURRENT CHARACTERISTICS AT 274m DEPTH.

5. TYPE OF REPORT & PERIOD COVERED: (9) Final rept.

6. PERFORMING ORG. REPORT NUMBER: (14) NAVTORPSTA-1311

7. AUTHOR(s): (10) Robert A. Helton, James R. Holbrook

8. CONTRACT OR GRANT NUMBER(s)

9. PERFORMING ORGANIZATION NAME AND ADDRESS:
Code 7023, Oceanography Branch
Applied Research Division
Research & Engineering Department

10. PROGRAM ELEMENT, PROJECT, TASK AREA & WORK UNIT NUMBERS

11. CONTROLLING OFFICE NAME AND ADDRESS: NAVSEASYSCOM

12. REPORT DATE: (11) May 1977

13. NUMBER OF PAGES: 82

14. MONITORING AGENCY NAME & ADDRESS (if different from Controlling Office): (12) 89p.

15. SECURITY CLASS. (of this report): UNCLASSIFIED

15a. DECLASSIFICATION/DOWNGRADING SCHEDULE

16. DISTRIBUTION STATEMENT (of this Report)

Approved for public release; distribution unlimited

17. DISTRIBUTION STATEMENT (of the abstract entered in Block 20, if different from Report)

18. SUPPLEMENTARY NOTES

*James R. Holbrook is at the Pacific Marine Environmental Laboratory of NOAA, 3711 15th Avenue NE, Seattle, WA 98005

19. KEY WORDS (Continue on reverse side if necessary and identify by block number)

tidal currents	along-range currents
harmonic constants	current prediction methods
cross-range currents	current measurement decision criteria

20. ABSTRACT (Continue on reverse side if necessary and identify by block number)

The current structure at 274m depth in the Nanoose test range was studied to determine component speeds along-range centerline and cross-range centerline. This followed an earlier investigation to delineate water layers with minimum motion. Decision criteria for determining the necessity of testing-support current measurement are presented.

TABLE OF CONTENTS

ACKNOWLEDGMENT

The authors are indebted to Dr. David Halpern for his continued interest in and support of coastal oceanography and to Andy Shepherd for his expert VACM preparation.

LIST OF FIGURES

LIST OF TABLES

1. INTRODUCTION

This report satisfies several objectives:

1. Provides decision-making criteria for determining whether current measurements are required to support device testing at the Nanoose Range. These criteria are supported by statistics which estimate the magnitude of the uncertainty in predicting the current field.

2. Reviews and illustrates the data-reduction and -analysis techniques that were performed to develop the decision-making criteria.

3. Describes the required data in terms of its acquisition methodology, quality, and references and describes other utilized data.

4. Summarizes the philosophy for the investigatory current measurements to the present time and makes recommendations for future data acquisition at the Nanoose Range and the Dabob Bay Range.

The report first introduces the reason for the investigatory current measurements. Following this the decision-making criteria for future measurement of current are presented. In the next two sections, the analysis of the data which supports the decision-making criteria are described. Included in these sections are discussions of water current prediction methodologies and descriptions of other utilized data. When self-contained descriptions are available they are included as appendices.

2. CURRENT MEASUREMENT PHILOSOPHY

In several instances there has been concern over the determination of what caused a device under test to veer from its programmed course or to be outside of its proofing specification end-of-run positional envelope.

Depending on the test geometry, two accumulative-type effects can cause these positional errors. In a static medium, device positional error can only be ascribed to the device. In a dynamic medium (in motion with respect to the bottom-mounted tracking system) positional error can also be caused by natural motions of the medium. Error can be nulled out or exaggerated by the water motion. Both of these effects are a function of run duration.

To increase knowledge of the test medium and decrease the risk of accepting devices not meeting specifications, a two-phase investigation was planned and implemented. The first phase entailed the monitoring of water current at several depths throughout the water column. This phase was completed in 1975. The reported results and investigation background are presented in Appendix A. It was determined that the cross-range and along-range (along-range is along range centerline) current magnitudes were jointly minimal at a depth of 900 feet. This observation, however, was based upon short periods of current measurements at one location and could vary both seasonally and spatially throughout the range.

The second phase, described in this report, entailed a 31-day measurement of water current at 900-foot (274m) depth with a vector-averaging current meter (VACM) and was aimed at achieving a predictive capability for current characteristics. If current could be predicted within suitable bounds, measurement would not be necessary. Time and money could therefore be saved.

3. DECISION CRITERIA FOR SPECIFYING MEASUREMENT OF CURRENT

INTRODUCTION

For various device testing either an end-of-run (EOR) positional error-circle or allowable deflection error is specified. The medium motion (water currents) and run time both influence this error. A knowledge of the uncertainty of the medium-induced offset is sufficient to enable the project engineer to decide whether current measurements are required for evaluation of device performance. Although a major conclusion of this report is "test the devic_ at 900 feet for minimum medium-induced offset," estimates for other depths are provided.

CRITERIA AT 900-FOOT DEPTH

From the measurements made during the 31-day period at 900-foot depth, Tables 1 and 2 were compiled. The tables show the maximum cross-range and along-range offsets to be expected at 95 and 80 per cent confidence intervals respectively. For example, Table 1 shows that for a 95 per cent confidence interval the cross-range offset will be no more than ±42 yards after 10 minutes of run time.

For any given test, <u>if</u> the offsets in Tables 1 and 2 are not acceptable, the current should be measured.

Table 1. Medium-Induced Offset
For a Two-Tailed 95% Confidence Interval
at 274m (900 feet) Depth

Run Time	Cross-Range (yd) σ = 3.2 cm/sec	Along Range (yd) σ = 7.2 cm/sec
10 min	42	93
30 min	124	278
1 hour	247	556
2 hours	494	1112
3 hours	741	1667

Table 2. Medium-Induced Offset
For a Two-Tailed 80% Confidence Interval
at 274m (900 feet) Depth

Run Time	Cross-Range (yd) σ = 3.2 cm/sec	Along-Range (yd) σ = 7.2 cm/sec
10 min	27	61
30 min	81	182
1 hour	162	363
2 hours	323	726
3 hours	484	1089

The range of uncertainty or the risk of exceeding the offsets tabulated in Tables 1 and 2 can possibly be reduced per section 5 of this report by use of additional information. The additional information entails current predictions using station 32 data and Winchelsea Island tide gauge data.

For the along-range offset, the standard deviation (σ) of the predicted current, utilizing station 32 harmonic constants, can possibly be reduced to 4.1 cm/sec from the Table 2 value of 7.2 cm/sec. A reduction in cross-range offset uncertainty can possibly be achieved through utilization of Winchelsea Island tide height information. The improvement results from a reduction in the predicted cross-range current standard deviation from a non-prediction value of σ = 3.2 cm/sec to a minimal value of σ = 2.6 cm/sec. The development of current-speed predictions by linear-regression analysis (equations (2) and (7) respectively for along-range and cross-range currents) is given in section 5 of this report. The qualifying word "possibly" results from the short data records available for analysis and observed seasonal effects (personal communication*).

TESTS AT OTHER DEPTHS

Definitive current data are presently lacking for depths other than 900 feet and in seasons other than mid-spring. An estimate of the peak current speeds at various depths is shown in Figure 1. This figure is taken from R&E Memo 222-76.[1] As noted it includes the 1975 VACM data (see Appendix A) and verified range instrumentation system historical data.

The range instrumentation system data were acquired during numerous short acquisition periods (minutes of averaged data)

---

* *Dr. Pat Crean, Institute of Oceanography, University of British Columbia, Vancouver, BC*

[1]Research & Engineering Department Memo 222-76, *Current Speeds at the Dabob Bay, Nanoose and BARSTUR Tracking Ranges and Effects on Mine Mark 60*, 11 May 1976

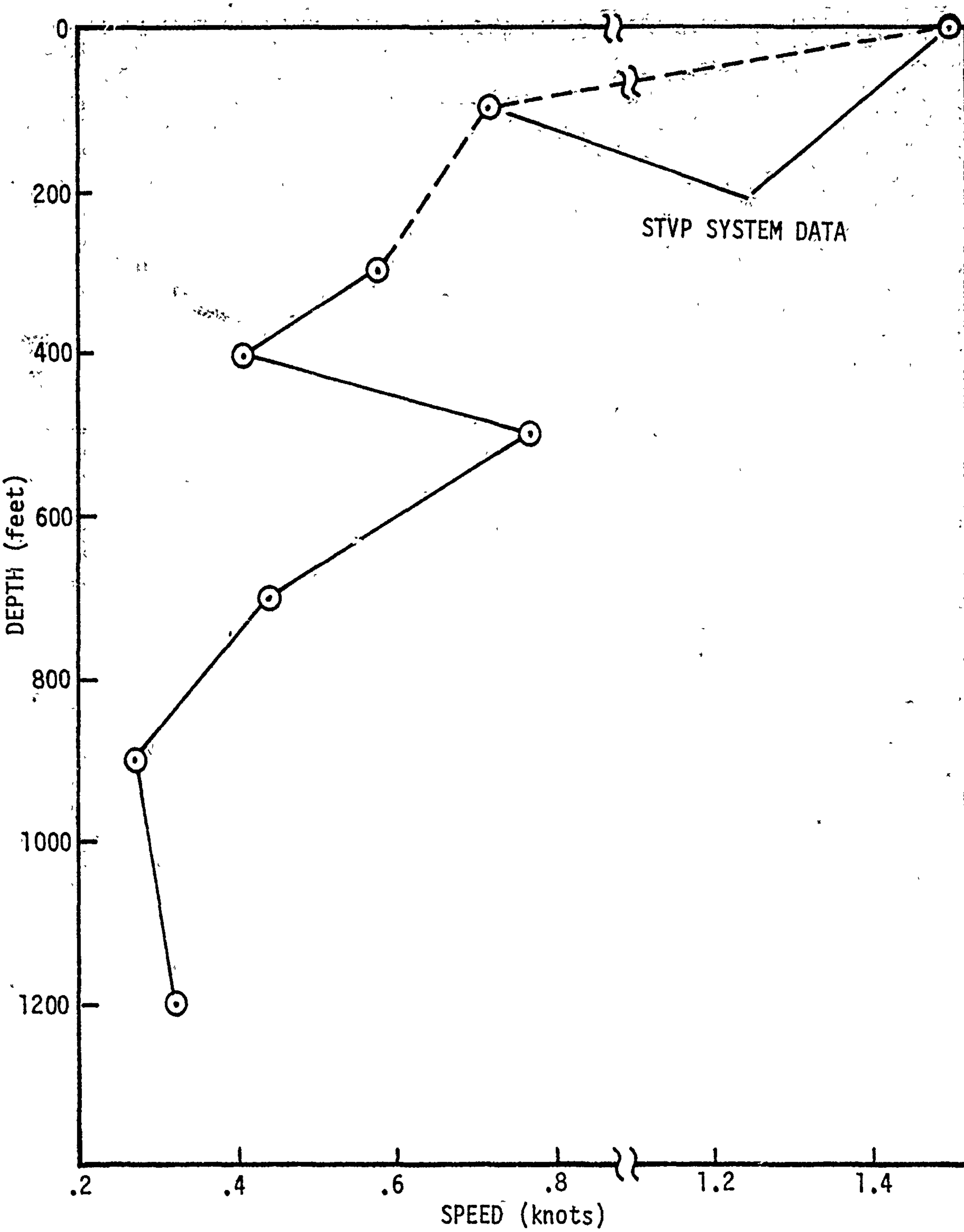

Figure 1. Peak Current Speeds from 1975 VACM and STVP System Data

over a span of several years for support of test programs. For these data only current speed is significant. The current-direction data are generally questionable because of low current speeds, measurement platform motions, and low data sampling rates. The range centerline spatial characteristics of these data are provided in Table 3. The peak STVP range system and the peak 1975 VACM measured currents are plotted in Figure 2 for comparison purposes.

Reliable directional data at several depths are in Table 4. These particular data, although indicative of what the current velocity can be, have minimal predictive use. For short-term measurements the current direction and the tidal phase characteristics are essentially not correlatable.

If the broad spans of possible along-range and cross-range currents in Table 4 are not acceptable, either the current should be measured or the device should be tested at 900-foot depth. It should be recalled that a steady 1 cm/sec cross-range current component will yield 6.56 yards of ranged device offset/deflection after a 10-minute run time.

PROPER MEASUREMENT OF CURRENT

The conditions for achieving proper current measurements to support in-water tests are a function of the running depth.

At depths shallower than 50 feet, wind-induced cross-range currents and measurement errors may exceed tidal current values. For long runs (distance- and time-wise) many sampling positions may be required for proper assessment of the effects of currents. A valuable discussion of measurement pitfalls is contained in *Practical Problems in the Direct Measurement of Ocean Currents*.[2] These pitfalls include error-producing mechanisms such as:

1. Ship pendulation (during single point moor),

2. Boundary layer effects caused by the hull,

3. Current direction errors caused by shipboard magnetic influence,

4. Tilt errors, and

5. Ship heaving- and rolling-induced errors.

If a VACM were deployed from a range craft, the number of VACM samples required to cancel the above errors would vary

[2] Paquette, R. G., *Practical Problems in the Direct Measurement of Ocean Currents*, Proceedings of the Symposium on Transducers for Oceanic Research, Marine Sciences Instrumentation, Vol. 2, Plenum Press, New York, 1963

Table 3. STVP Range-System Measured Current Speed Characteristics

Depth Span (ft)	Range ℄ Span (yd)	Date Span	Sample Size	Mean Current Speed, μ (kn)	Variance (var)	$\mu+3\sqrt{Var}$	Peak Current Date Observed	Peak Current Speed (kn)
Surface to 28	8,400 18,900	8/25/70 10/24/74	38	0.56	0.119	1.59	5/10/73	1.55
87 to 113	10,300 16,400	8/12/70 12/13/73	6	0.50	0.058	1.23	8/ 1/73	0.86
200 to 212	12,000 15,000	8/ 7/70 4/23/71	8	0.52	0.077	1.35	4/18/71	0.91
284 to 315	14,600 16,950	5/10/73 8/29/74	8	0.17	0.021	0.60	8/ 1/73	0.46
390 to 406	9,750 18,900	6/ 7/72 12/20/74	8	0.24	0.011	0.55	12/21/72	0.38
492 to 520	9,750 18,200	3/21/73 5/ 1/74	4	0.32	0.064	1.08	9/13/73	0.74
589 to 615	11,100 16,400	5/10/73 6/ 8/74	5	0.19	0.007	0.44	5/10/73	0.30
880 to 921	14,600 16,400	5/ 6/71 5/31/74	5	0.10	0.002	0.23	5/ 6/71	0.15
1,023 to 1,086	15,000 23,000	4/13/71 6/30/71	9	0.21	0.016	0.59	4/19/71	0.50
1,119 to 1,285	11,100 16,950	8/17/70 8/29/74	20	0.20	0.009	0.47	4/18/73	0.33

Table 4. Range of VACM-Measured Currents at Various Depths

Greenwich Mean Time M=March, A= April 1975	Depth (ft)	Component Cross-Range (cm/sec)[a]	Component Along-Range (cm/sec)[a]
2100/31M to 1900/ 1A	100	-10 to +16	- 5 to +18
2300/ 1A to 1700/ 4A		-10 to +15	-22 to + 8
0200/22A to 1600/22A		- 9 to ~ 0	0 to +15
2300/22A to 1500/23A		-11 to +1.5	- 8 to +12
0100/24A to 1800/24A		- 7 to + 9	- 8 to +13
0000/25A to 1700/25A		- 9 to +10	-13 to + 8
2200/ 7A to 1700/ 9A	200	- 3 to +11	~ 0 to +19
2300/ 9A to 1700/10A		- 5 to + 4	0 to +18
2300/10A to 1600/11A		- 4 to + 4	0 to +17
2200/28A to 1500/29A		-13 to + 3	- 3 to +15
2300/29A to 1700/30A		- 9 to + 4	- 4 to +12
2200/30A to 1500/ 1M		- 5 to + 8	- 9 to +12
2300/ 1M to 1800/ 2M		- 6 to + 6	- 2 to +14
1700/15A to 1700/18A	300	- 6 to +6.5	-10.5 to +11
2200/25A to 2100/28A		-11 to +13	-12 to +27
1800/ 4A to 1800/ 7A	400	- 6 to +10	-20 to + 6
1500/29M to 0900/31M	500	0 to +20	-33 to 0
2300/11A to 1700/14A	600	-10 to +10	-19 to + 6
2100/14A to 1700/15A	700	~ 0 to + 5	-20 to 0
1900/18A to 1500/21A	1200	-7.5 to + 4	-14 to + 6

[a] *1 cm/sec for 10 minutes = 6.56 yards offset*

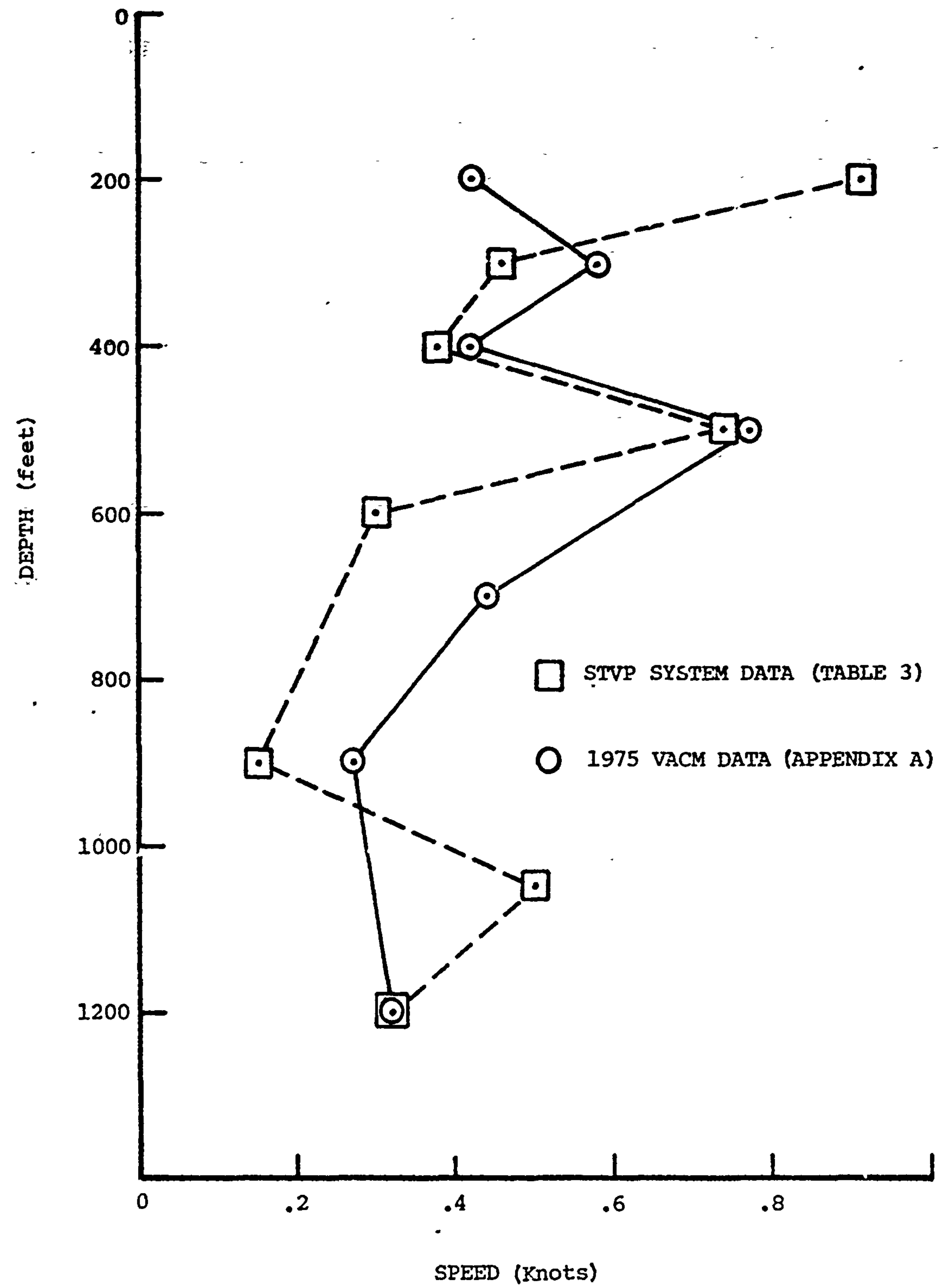

Figure 2. Peak Current Speeds Compared

with the circumstances encountered during the measurement period.

At depths greater than 50 feet, less probing of the medium is required. Again, however, avoidance or minimization of platform-induced error is always desirable.

4. SUPPORTING DATA AND ANALYSIS

INTRODUCTION

For the 31-day test the VACM was deployed by the Station's Bottom-Mounted Instrumentation System (BOMIS).

At 1528 local daylight time (LDT) on 18 May 1976, the BOMIS I buoy, with the VACM and subsurface float per Figure 3, was submerged to 274m depth, to remain for the 31 days as per run plan 9160 (see Appendix B). A continuous current speed and direction record for predicting the current at 274m depth was acquired. On 18 June Messrs. J. Eliason and R. Helton observed the recovery operation and noted the VACM data tape end-of-record vane-reversal event at 0937 LDT per the Winchelsea Island computer range clock time.

Analysis of this data record in conjunction with earlier results (see Appendix A) verified the previously indicated jointly minimal along-range and cross-range water currents at 274m depth. The following sections and appendices will present acquired data characteristics and discuss the applicability and limitations of water current prediction methods at 274m depth at the Nanoose Range. Figure 4 illustrates the measurement device (VACM) and the BOMIS I range equipment.

VACM DATA ACQUISITION AND REDUCTION

The VACM was preset to vector average the water current characteristics for 112.5-second periods. The VACM theory of operation and other pertinent characteristics are described in the *Vector Averaging Current Meter* manual,[3] NOAA-TM-NOS-NOIC-1,[4] and NOAA-TM-NOS-NOIC-3.[5] Each internally-recorded data point is the resultant vector summation of the actual current sampled every 1/8 turn of the Savonius rotor speed sensor over a 112.5-second period. This scheme can effectively filter out mooring motion noise (see Deep-Sea Research 21[6] and Deep-Sea Research 23[7]).

---

[3] *Vector Averaging Current Meter Model 610* manual, AMF Electrical Products Development Division, September 1973

[4] NOAA-TM-NOS-NOIC-1, *Report on the Evaluation of a Vector Averaging Current Meter*, William E. Woodward and Gerald F. Appel, July 1973

[5] NOAA-TM-NOS-NOIC-3, *Effects of Vertical Motion on Vector Averaging (Savonius Rotor) and Electromagnetic Type Current Meters*, A. N. Kalvaitis

[6] Deep-Sea Research 21, *An Intercomparison of Three Current Meters Operating in Shallow Water*, D. Halpern and others, pp 489-497, 1974

[7] Deep-Sea Research 23, *Near Surface Current Measurements*, P.M. Saunders, pp 249-258, 1976

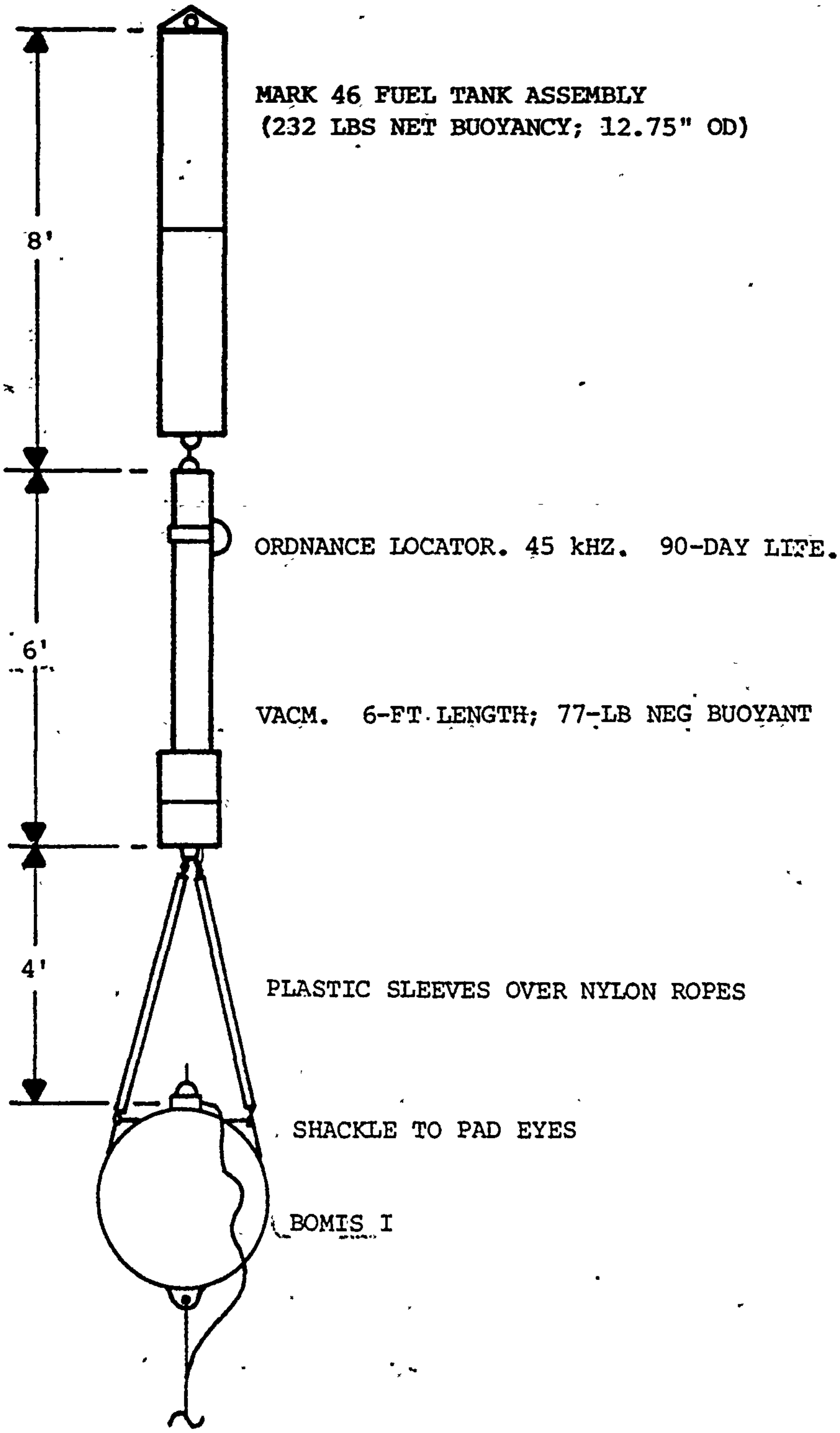

Figure 3. VACM Installation Atop BOMIS

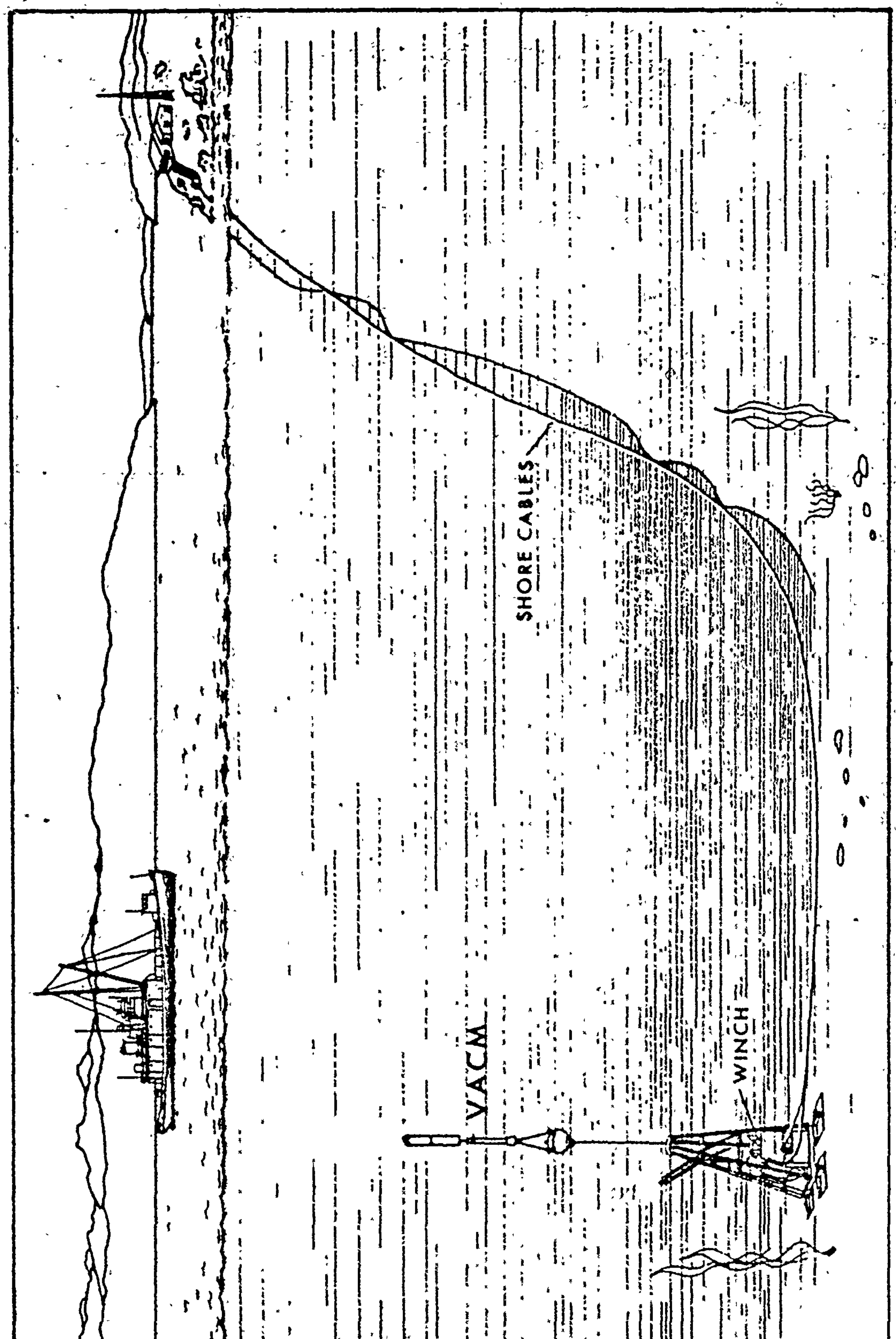

Figure 4. VACM Deployment Using BOMIS I

The data points were computer processed and resolved as before (see Appendix A) so a 0° direction implied the +Y range coordinate direction. Further data reduction averaged 16 of the 112.5-second vector averages to yield a mean characteristic for a 1/2-hour period. During the course of the VACM deployment period a 100 per cent valid data record was obtained. This provided 1,471 1/2-hour data periods on which to assess the current characteristics.

A loan of a VACM and data reduction was the result of a joint interest in currents in the Strait of Georgia between the Ocean Atmosphere Response Studies (OARS) group at the Pacific Marine Environmental Laboratory (PMEL) and NAVTORPSTA Keyport oceanography branch personnel. The particular NAVTORPSTA interest entailed the search for a water layer of minimum motion at the Nanoose Range (phase 1) and predictive definitization of this motion (phase 2).

WATER CURRENT CHARACTERISTICS AT 274m DEPTH

Histograms of 1/2-hour averaged speed and direction of currents for the 31-day data set are shown in Figures 5 and 6. The mean current speed throughout the acquisition period was 6.9 cm/sec (1 knot = 51.48 cm/sec). Ebb and flood directions centered around 105° and 285° relative to the +Y axis. These directions are 118°TN (true north) and 298°TN respectively.

Directional fans for speeds greater than 9 cm/sec are shown in Figure 7. There were 239 and 121 1/2-hour averaged data points to define the flood and ebb fans respectively in Figure 7. In only 360 of 1,471 events (or less than 25 per cent of the time) did the 1/2-hour averaged current speed exceed 9 cm/sec. Table 5 summarizes the component current speed data characteristics and Figure 8 illustrates the resolved along-range and cross-range component current characteristics. A time-partitioned histogram of the data is provided in Appendix C to illustrate current characteristic variations.

Table 5. Observed Component Current Speeds

Along-Range Component, U		Cross-Range Component, V	
cm/sec	Ratio Events/Total	cm/sec	Ratio Events/Total
>10	232/1471 = 15.8%	>5	212/1471 = 14.4%
>15	49/1471 ≐ 3.3%	>8	3/1471 = 0.2%

In Figure 8 the +Y or cross-range direction and the +X or along-range directions are 13° and 103°TN respectively. The plotted direction is referenced to the 12 o'clock high or +Y axis direction. The next two panels illustrate the resolved along- and cross-range current velocities. The bottom panel in Figure 8 illustrates via a stick diagram the 24-hour running mean current characteristics. The length of the stick or vector is current and its direction is the angular direction relative to range centerline.

LOCATION = LAT 49 19.8N, LONG 124 2.1W, DEPTH = 274 METERS
OBSERVATION PERIOD = 2330 18 MAY 76 TO 1400 18 JUN 76 (30.6 DAYS)
N = 1470, DT = 30.00 MINUTES, UNITS = (CM/SEC) (TIMES ARE GMT)

	MEAN	VARIANCE	ST-DEV	SKEW	KURT	MAX	MIN
S	6.89	15.11	3.89	.695	3.448	20.59	.00
U	-.84	51.13	7.15	-.123	2.531	18.96	-20.04
V	.68	10.35	3.22	-.177	2.445	8.39	-8.34

S = SPEED
U = ALONG-RANGE COMPONENT OF VELOCITY, 103°TN = POSITIVE U
V = CROSS-RANGE COMPONENT OF VELOCITY, 13°TN = POSITIVE V

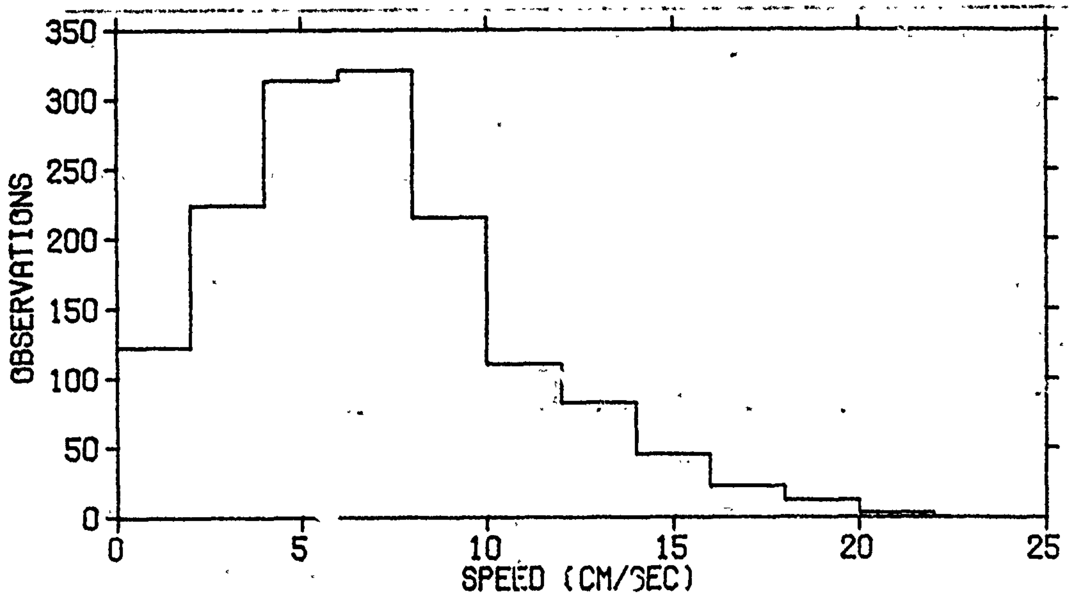

Figure 5. Histogram of 31-Day-Period Current Speeds

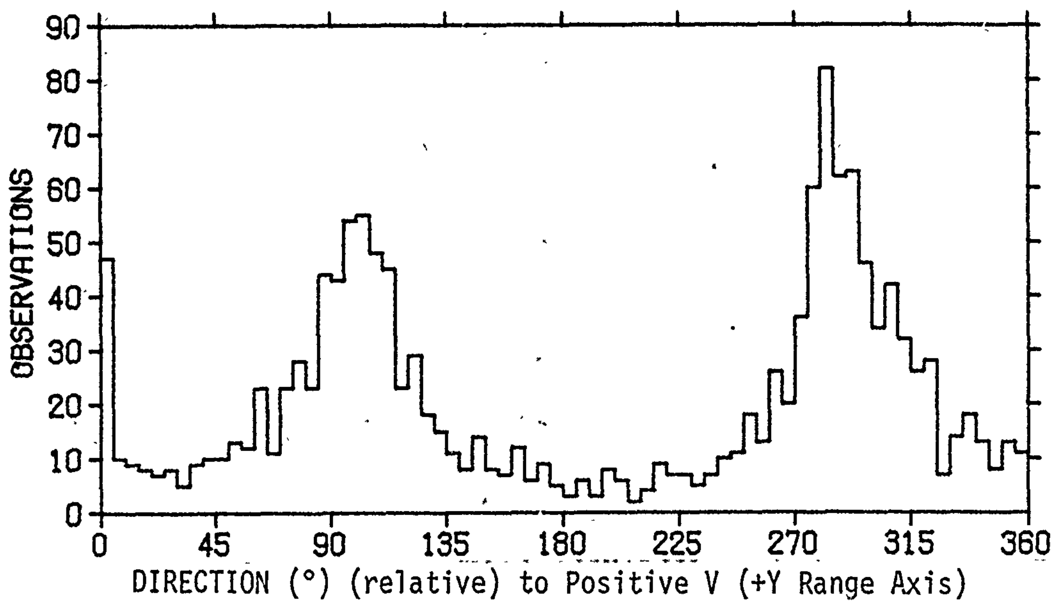

Figure 6. Histogram of 31-Day-Period Current Directions

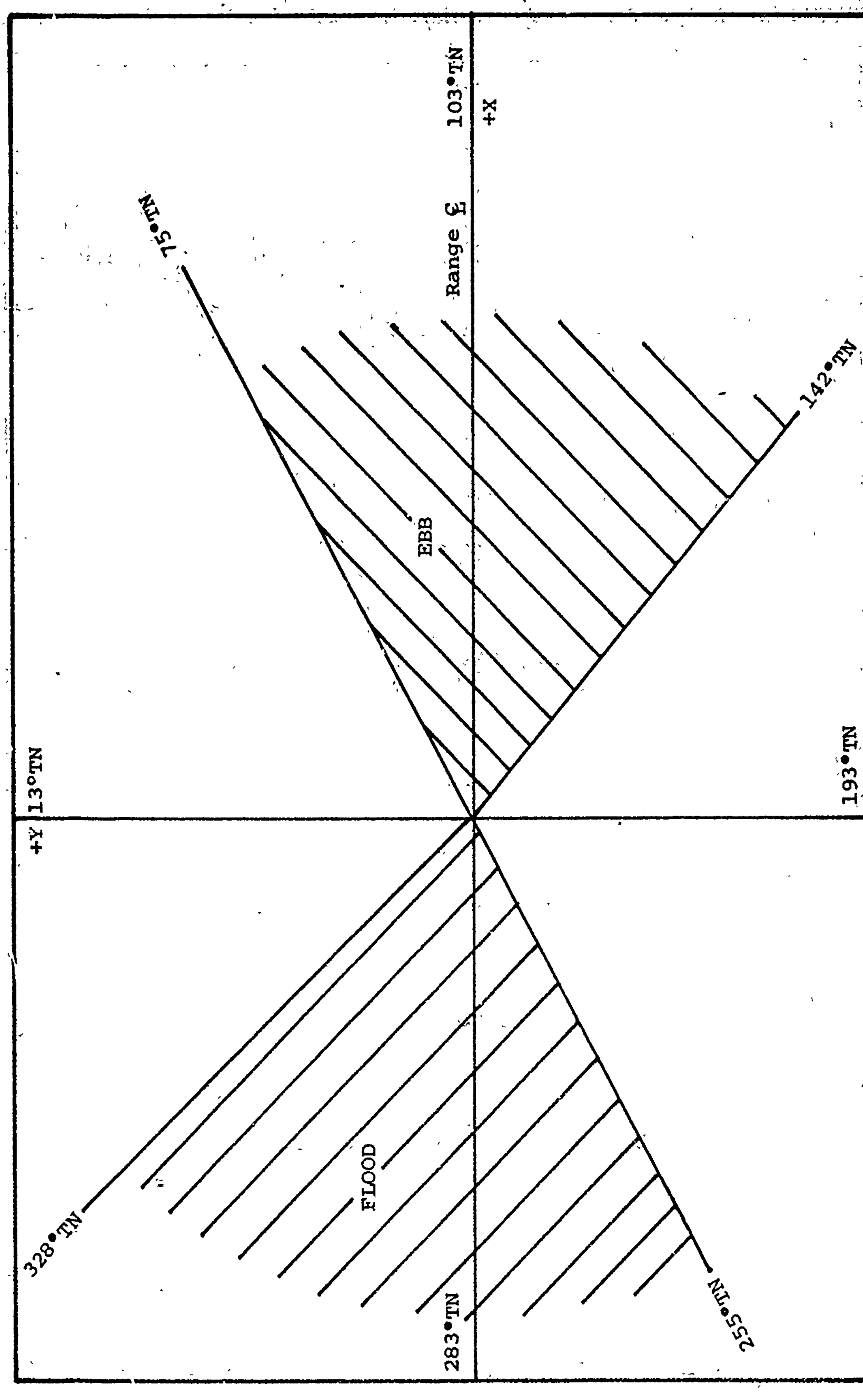

Figure 7. Directional Fans for Speeds >9 cm/sec at 274m Depth

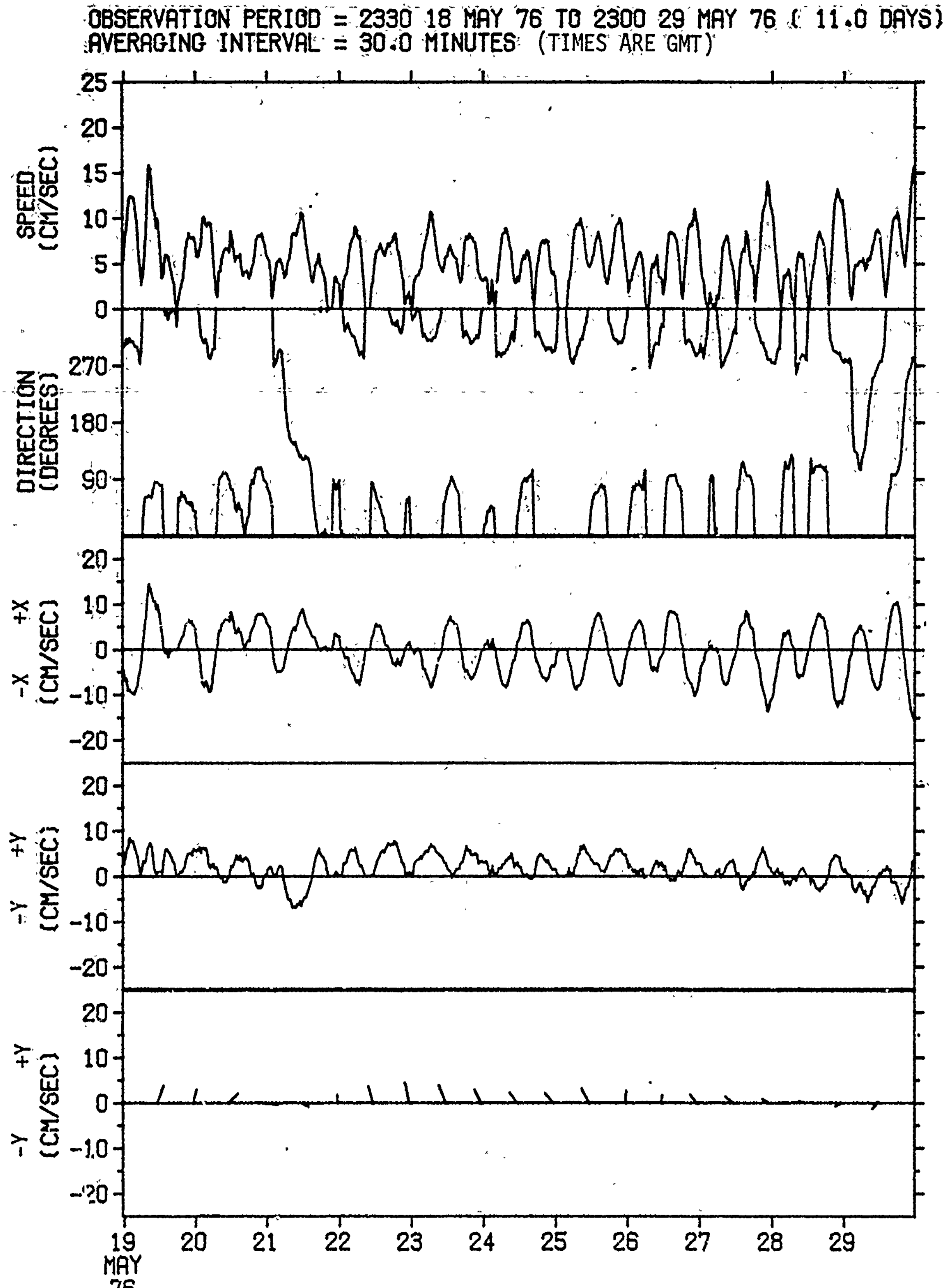

Figure 8. Time Series of Vector-Averaged Currents at BOMIS, 1976 (beginning)

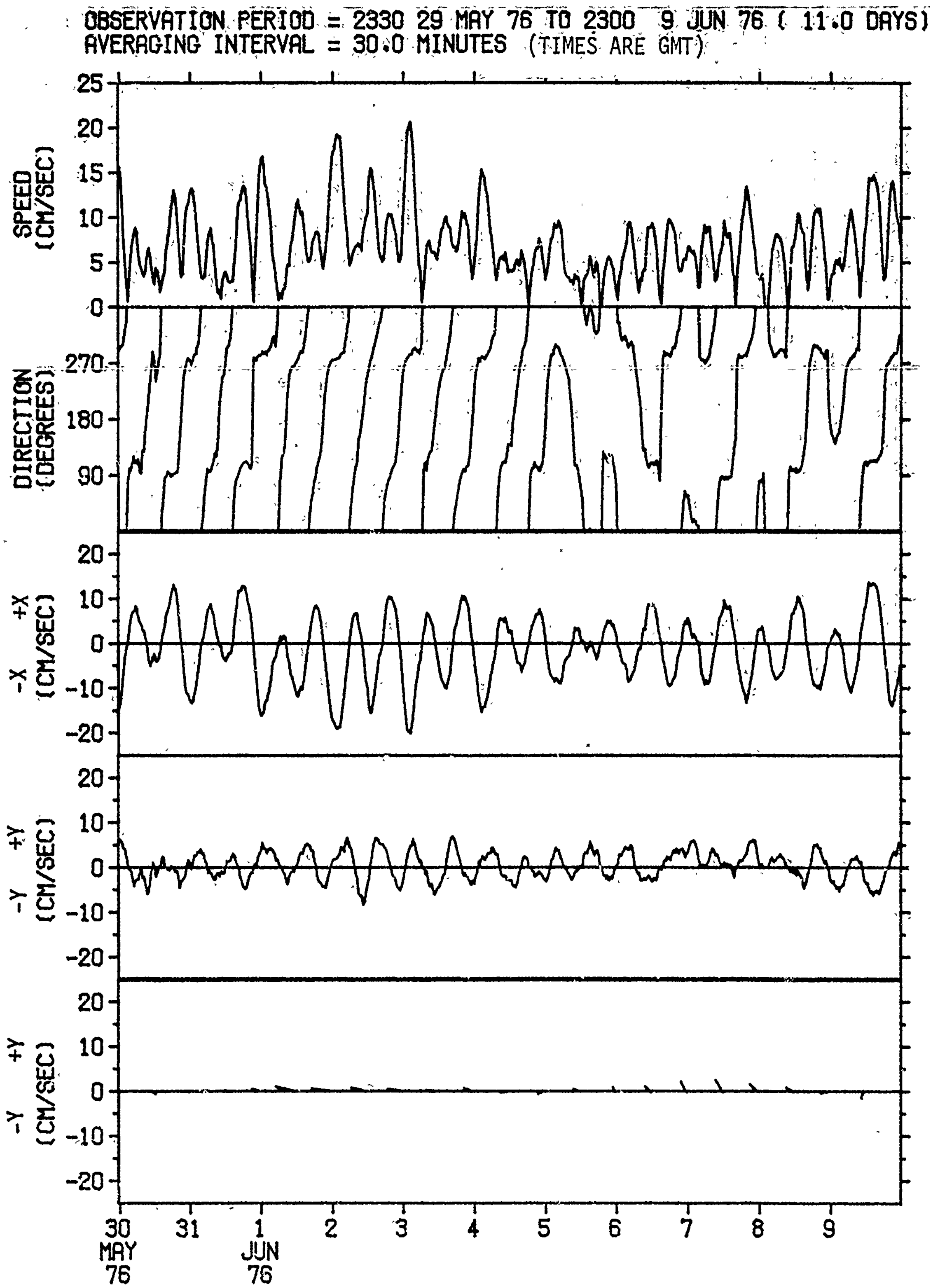

Figure 8. Time Series of Vector-Averaged Currents at BOMIS, 1976 (continued)

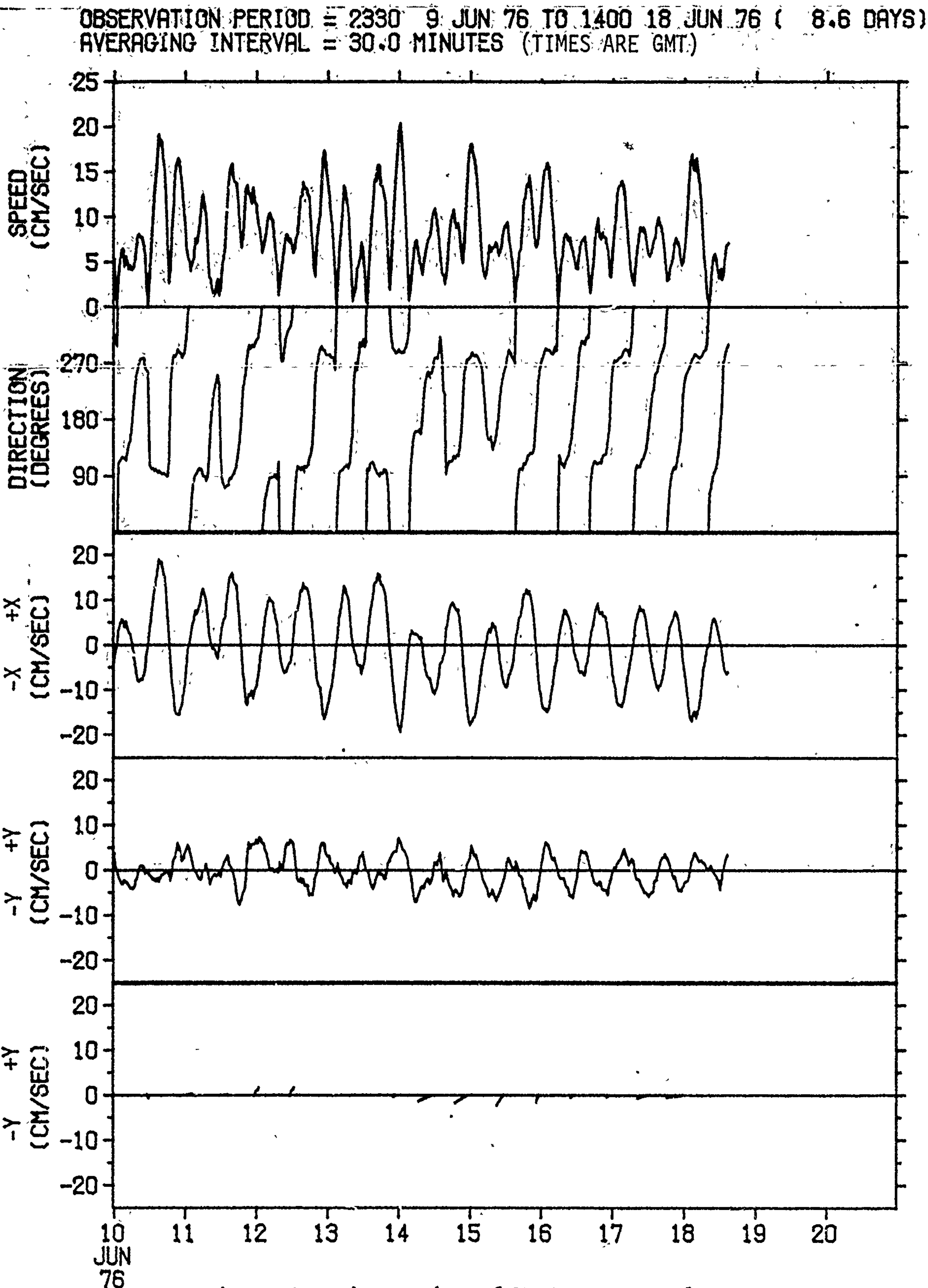

Figure 8. Time Series of Vector-Averaged Currents at BOMIS, 1976 (concluded)

5. WATER CURRENT PREDICTION METHODS

INTRODUCTION

In this section, two basic methods of current prediction are examined. The first utilizes previously computed tidal harmonic constants (based on current measurements made by Environment Canada at two nearby stations) to generate predictions. Recent current measurements at the BOMIS I site (49°19.8'N,124°02.1'W) are compared with these predictions. The second method involves linear regression techniques which correlate the measured currents at the BOMIS I site with tidal height data recorded at Winchelsea Island. The residuals about this regression are used to estimate the confidence interval that may be attached to this prediction method.

Figure 9 illustrates the distribution of energy of the along-range (103°TN) and cross-range (13°TN) components of current at 274m depth at the BOMIS I site. Table 6 summarizes the partition of energy into the low-frequency (periods >35 hours), and tidal (diurnal and semi-diurnal) regimes. The

Table 6. Distribution of Energy at 274m Depth at BOMIS I Site
(Numbers in parenthesis represent relative per cent)

Component	Period (hr)	Along-Range (%)	Cross-Range (%)
Low frequency	>35	5.8 *(7.0)*	4.0 *(23.8)*
Diurnal	23.0-26.3	11.9 *(14.3)*	0.9 *(5.4)*
Semi-diurnal	11.8-12.9	58.8 *(70.7)*	6.9 *(41.1)*
Remainder (noise[a])	-	6.7 *(8.1)*	5.0 *(29.7)*
TOTAL	-	83.2 *(100.0)*	16.8 *(100.0)*

[a]*Natural, unexplained higher frequency motion*

along-range component contains 83 per cent of the total energy of the water fluctuations. Of this along-range energy, 7 per cent is low frequency, 14 per cent is diurnal, and 71 per cent is semi-diurnal. The remainder (8 per cent) can be considered as noise* which is spread throughout the higher-frequency portion of the spectrum.

**Noise is defined as natural, unexplained, higher frequency motion.*

OBSERVATION PERIOD = 2330 18 MAY 76 TO 1400 18 JUN 76 (30.6 DAYS)
N = 1470, DT = 30.00 MINUTES, SMOOTHING = DANIELL WINDOW

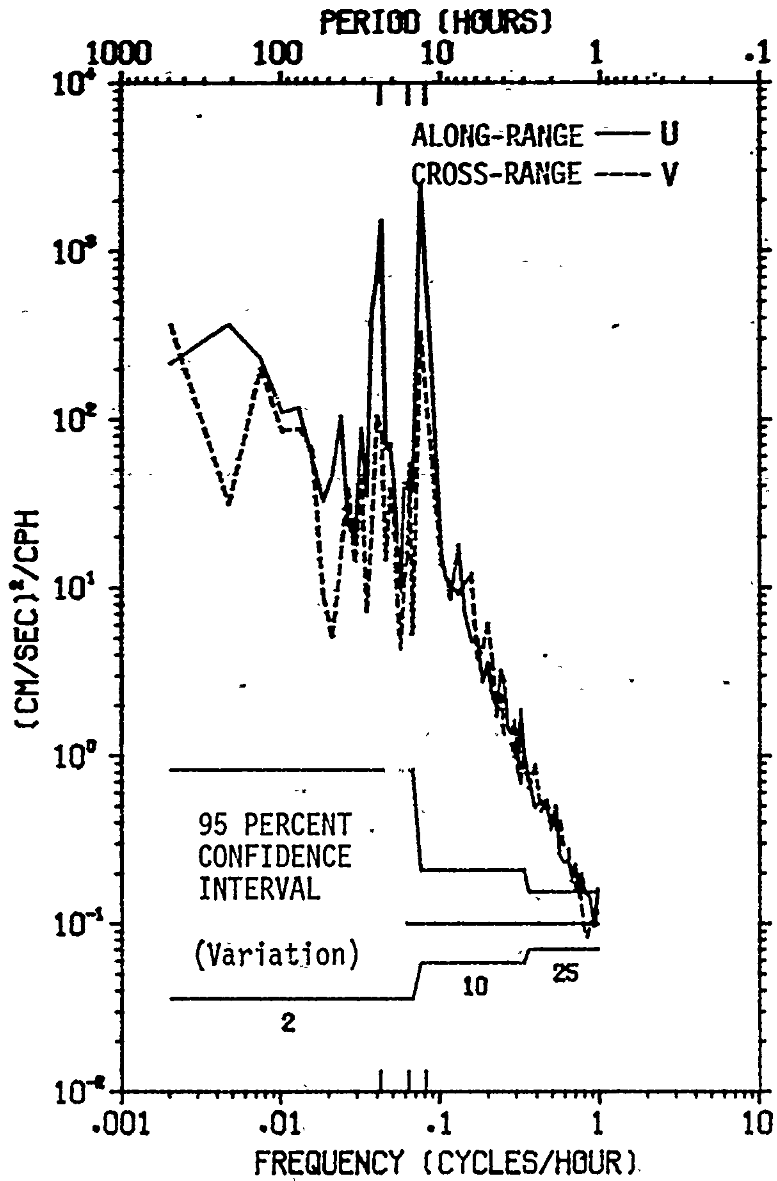

Figure 9. U and V Spectra of Currents at BOMIS, 1976

Of the cross-range energy, 24 per cent is low frequency, 5 per cent is diurnal, 41 per cent is semi-diurnal, and 30 per cent is noise. Thus the tides (primarily the semi-diurnal constituent) dominate the current record, accounting for approximately 78.5 per cent of the total energy. The prediction methods to be discussed are based principally on this tidal energy.

The low-frequency motions (which account for approximately 10 per cent of the total energy) may be isolated by low-pass filtering of the original current record with a numerical filter as described by Godin's *Analysis of Tides*.[8] This filter has a half-power cut-off period of 90 hours and is designed to remove diurnal and semi-diurnal tidal energy. Figure 10 shows the along-range (top) and cross-range (bottom) 30-minute-averaged and low-pass-filtered time series. The amplitude of the low-frequency oscillations varies from -4.5 to 2.6 cm/sec along range and from -1.7 to 3.7 cm/sec cross range. Low-frequency speeds greater than 3 cm/sec occur from 1030 Local Greenwich Meridian Time (LGMT) 22 May to 0430 LGMT 24 May (42 hours), from 0430 LGMT 1 June to 0030 LGMT 3 June (44 hours), and from 1430 LGMT 14 June to 0230 LGMT 15 June 1976 (12 hours). Typically these long-period fluctuations are attributed to variations in the surface wind stress, in the atmospheric pressure field, and in the thermohaline (estuarine) circulation. Prediction of these motions is not presently possible, since the data record is insufficient and since seasonal effects are known to exist.

Histograms and normal probability characteristics distribution of the along-range and cross-range components of current velocity are shown in Figures 11, 12, 13, and 14. Tabular data for these figures are provided in Tables 7 and 8.

An estimate of the lower limit of the 95 per cent confidence interval associated with any prediction method based upon tidal energy can be calculated by totaling the non-tidal variance, i.e., integrating the non-tidal spectral estimates shown in Figure 9 from a tabulated computer listing (see Holbrook and Halpern's VECPLOT[9]), and computing the 2σ interval. (Such an estimate assumes the non-tidal variance to be normally distributed.) For the along-range and cross-range components, such a lower limit would be ±5.6 cm/sec and ±4.7 cm/sec, respectively (2σ limits). Until these non-tidal motions are

[8] *The Analysis of Tides*, Gabriel Godin, University of Toronto Press, 1972

[9] *VECPLOT: A Graphics Program to Display Current and Wind Time-Series Data*, J. R. Holbrook and D. Halpern, Proceedings of the Working Conference on Oceanographic Data Systems, Woods Hole Oceanographic Institution, pp 217-232, 1975

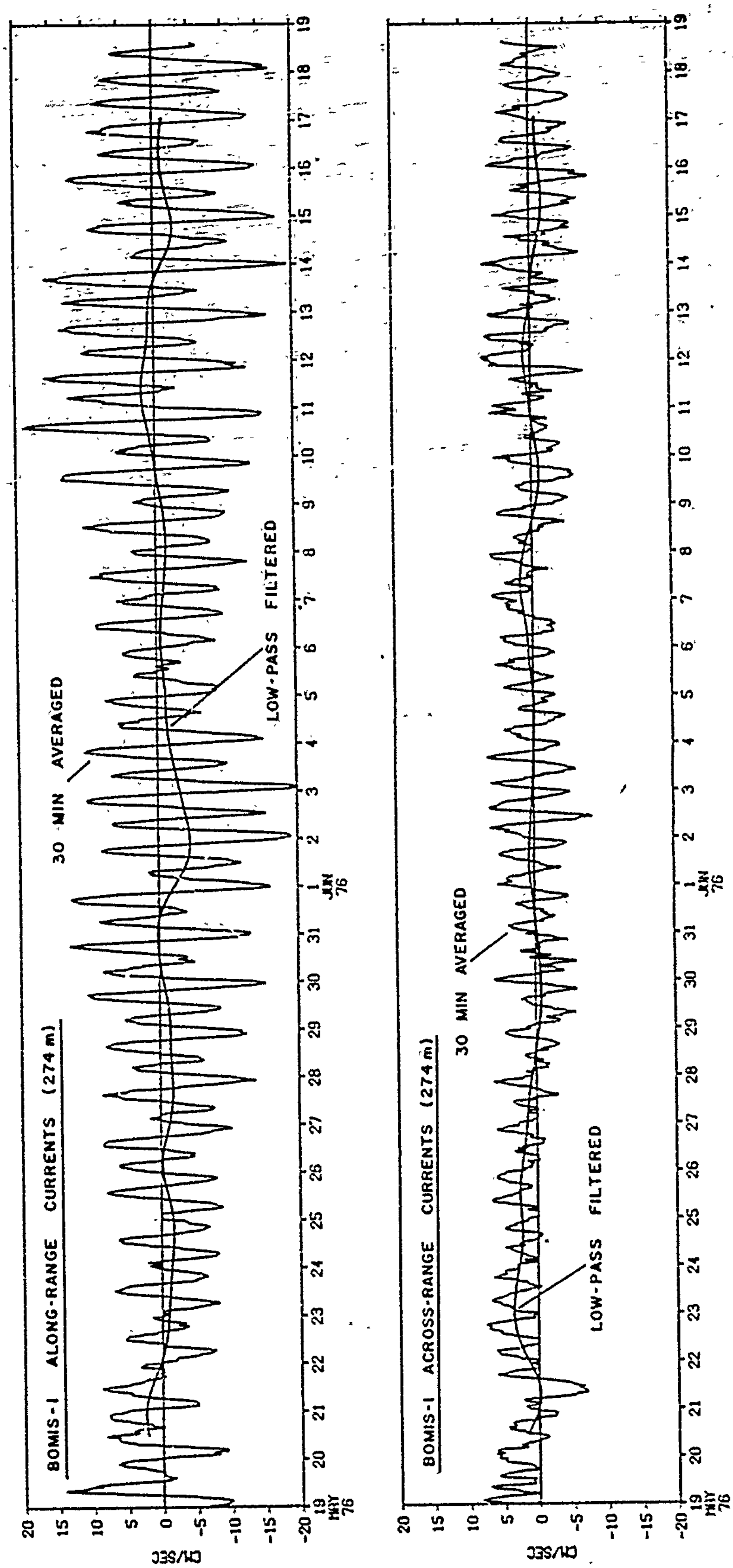

Figure 10. Time Series of Averaged and Low-Pass Filtered Data at BOMIS I

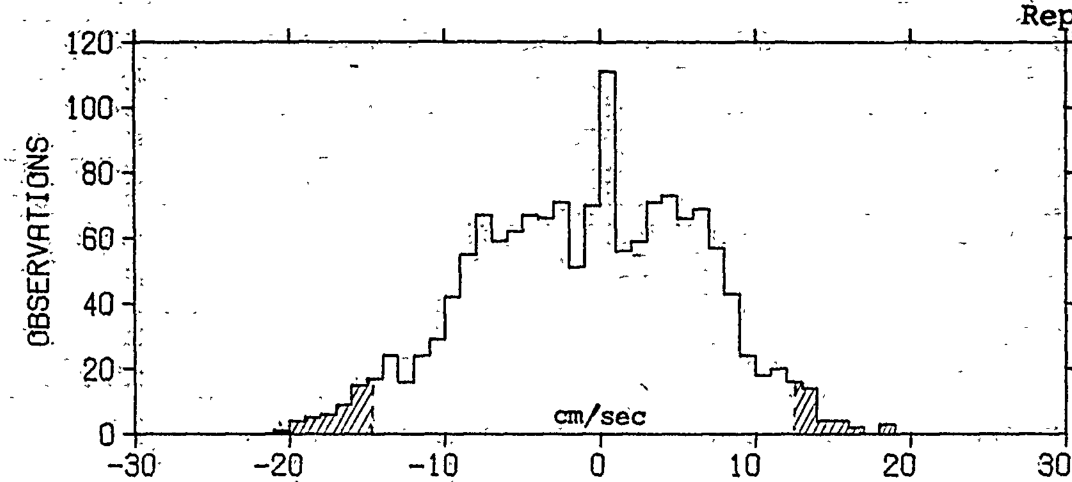

Figure 11. Histogram for Along-Range Currents

Table 7. Histogram Values for Figure 11

Class Interval (cm/sec)	Events	%	Cumulative %
-21.0 to -20.0	1	.1	.1
-20.0 to -19.0	4	.3	.4
-19.0 to -18.0	5	.3	.7
-18.0 to -17.0	6	.4	1.1
-17.0 to -16.0	9	.6	1.7
-16.0 to -15.0	15	1.0	2.7
-15.0 to -14.0	17	1.2	3.9
-14.0 to -13.0	24	1.6	5.5
-13.0 to -12.0	16	1.1	6.6
-12.0 to -11.0	24	1.6	8.2
-11.0 to -10.0	29	2.0	10.2
-10.0 to - 9.0	42	2.9	13.1
- 9.0 to - 8.0	55	3.7	16.8
- 8.0 to - 7.0	67	4.6	21.4
- 7.0 to - 6.0	59	4.0	25.4
- 6.0 to - 5.0	62	4.2	29.6
- 5.0 to - 4.0	67	4.6	34.2
- 4.0 to - 3.0	66	4.5	38.7
- 3.0 to - 2.0	71	4.8	43.5
- 2.0 to - 1.0	51	3.5	47.0
- 1.0 to .0	70	4.8	51.8
.0 to 1.0	111	7.6	59.4
1.0 to 2.0	56	3.8	63.2
2.0 to 3.0	59	4.0	67.2
3.0 to 4.0	71	4.8	72.0
4.0 to 5.0	73	5.0	77.0
5.0 to 6.0	66	4.5	81.5
6.0 to 7.0	69	4.7	86.2
7.0 to 8.0	57	3.9	90.1
8.0 to 9.0	43	2.9	93.0
9.0 to 10.0	24	1.6	94.6
10.0 to 11.0	18	1.2	95.8
11.0 to 12.0	20	1.4	97.2
12.0 to 13.0	16	1.1	98.3
13.0 to 14.0	14	1.0	99.3
14.0 to 15.0	4	.3	99.6
15.0 to 16.0	4	.3	99.9
16.0 to 17.0	2	.1	100.0
17.0 to 18.0	0	.0	100.0
18.0 to 19.0	3	.2	100.2

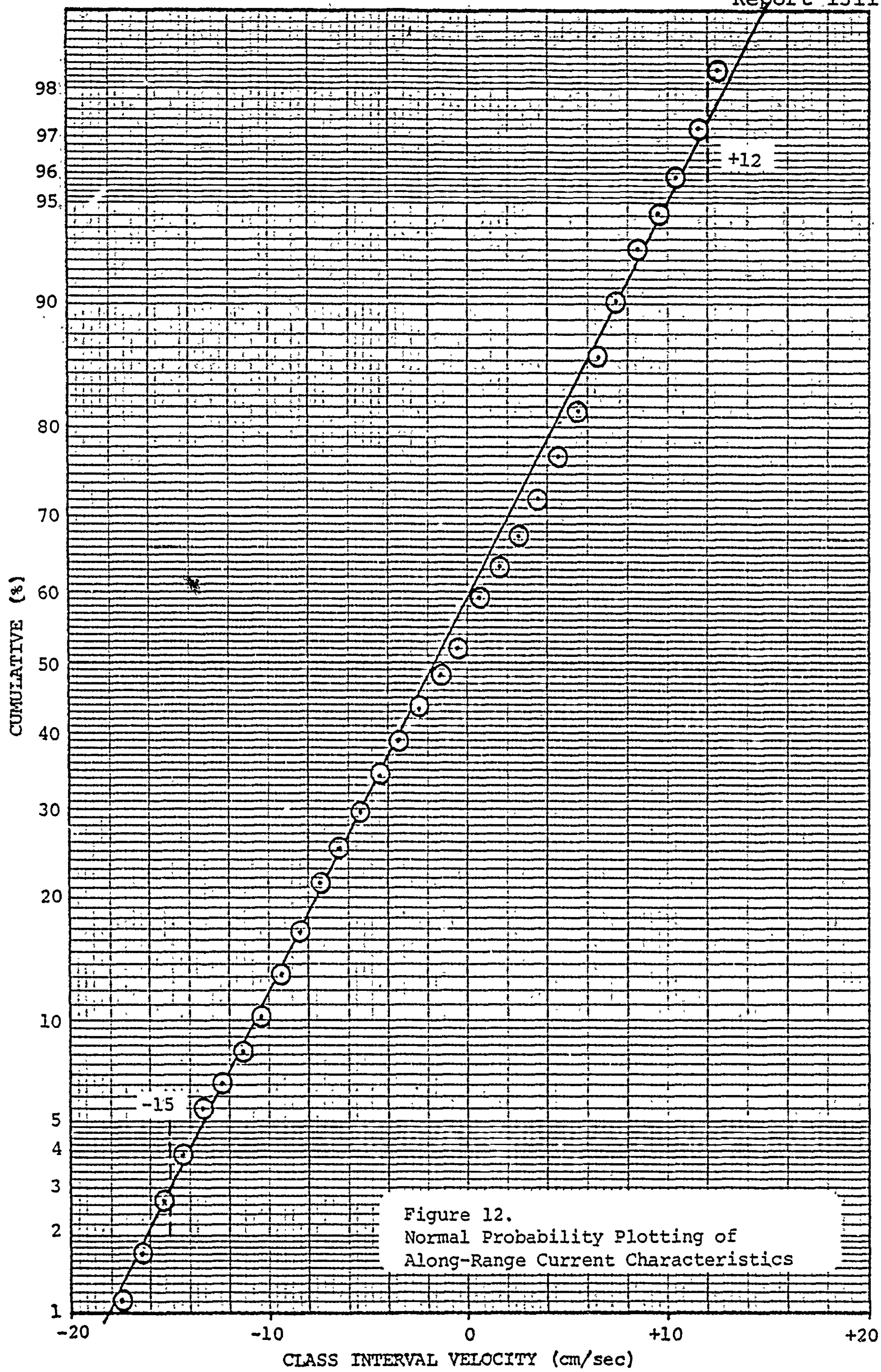

Figure 12.
Normal Probability Plotting of
Along-Range Current Characteristics

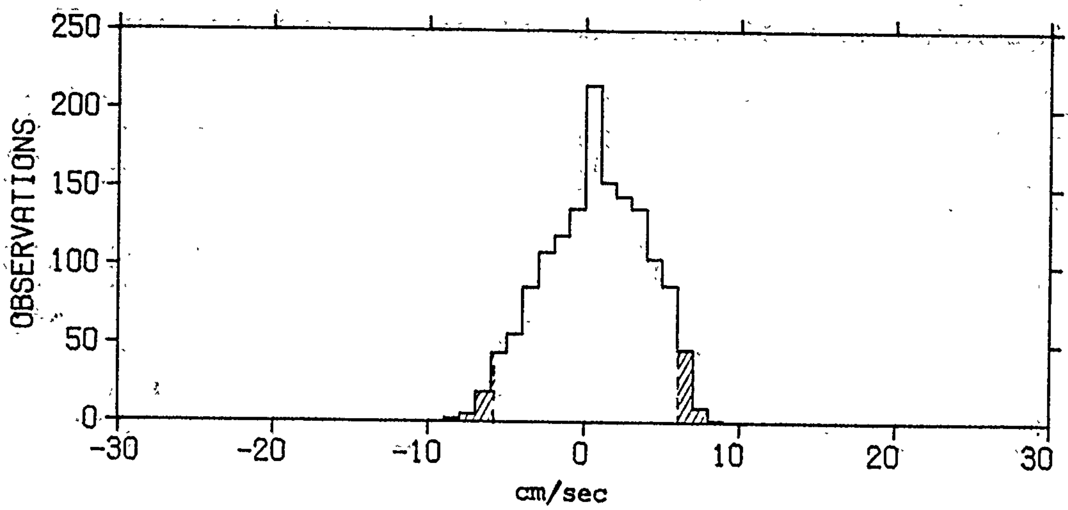

Figure 13. Histogram for Cross-Range Currents

Table 8. Histogram Values for Figure 13

Class Interval (cm/sec)	Events	%	Cumulative %
-11.0 to -10.0	0	.0	
-10.0 to - 9.0	0	.0	0.0
- 9.0 to - 8.0	2	.1	.1
- 8.0 to - 7.0	5	.3	.4
- 7.0 to - 6.0	19	1.3	1.7
- 6.0 to - 5.0	44	3.0	4.7
- 5.0 to - 4.0	56	3.8	8.5
- 4.0 to - 3.0	86	5.9	14.4
- 3.0 to - 2.0	108	7.3	21.7
- 2.0 to - 1.0	119	8.1	29.8
- 1.0 to .0	136	9.3	39.1
.0 to 1.0	215	14.6	53.7
1.0 to 2.0	153	10.4	64.1
2.0 to 3.0	144	9.8	73.9
3.0 to 4.0	136	9.3	83.2
4.0 to 5.0	104	7.1	90.3
5.0 to 6.0	87	5.9	96.2
6.0 to 7.0	46	3.1	99.3
7.0 to 8.0	9	.6	99.9
8.0 to 9.0	1	.1	100.0
9.0 to 10.0	0	.0	
10.0 to 11.0	0	.0	

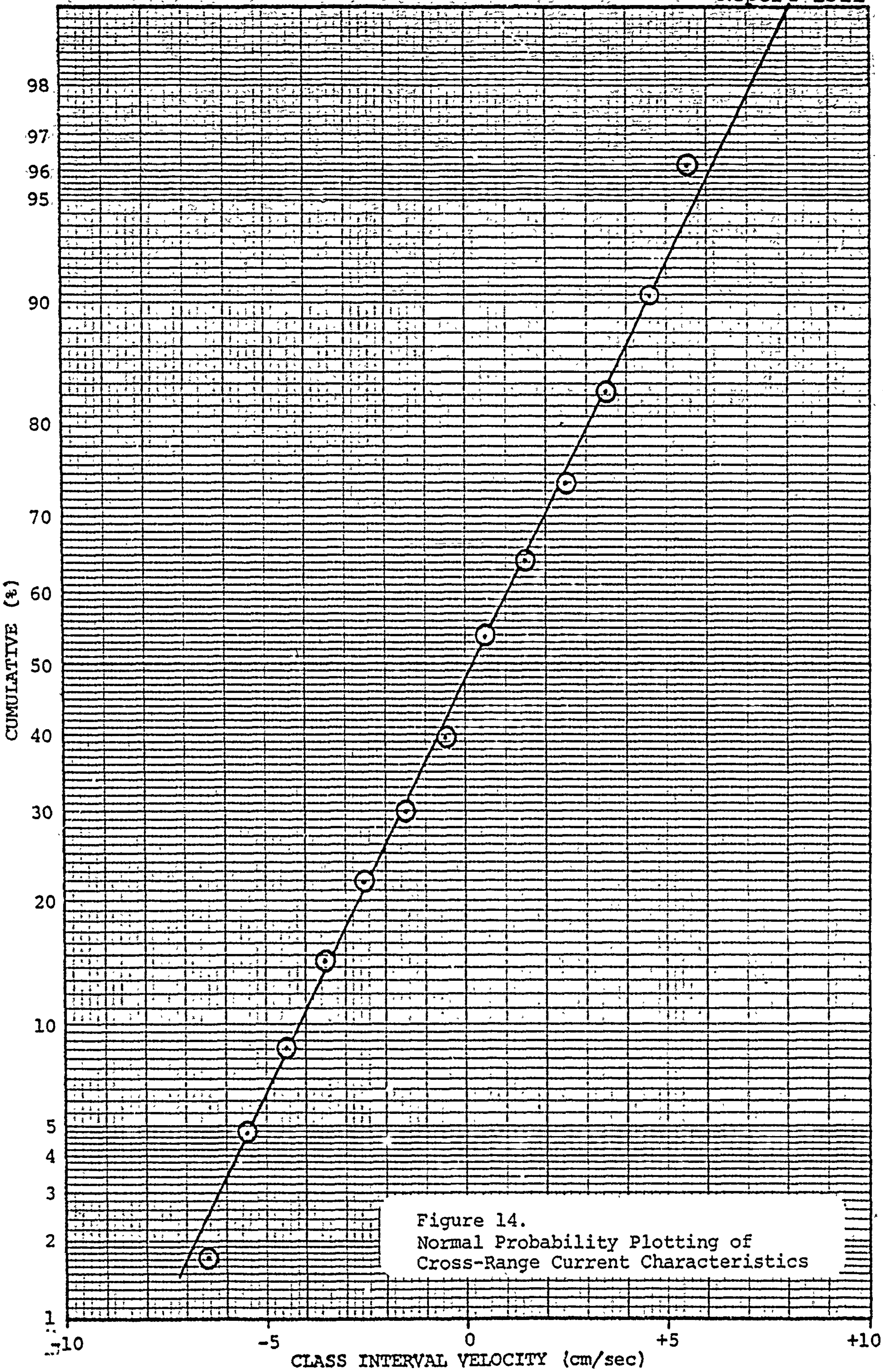

Figure 14.
Normal Probability Plotting of
Cross-Range Current Characteristics

better understood the best possible tide-based prediction can be no better than the constraints imposed by the above variance limits.

HARMONIC CONSTANT METHOD

Current measurements were made by Environment Canada at Station 32 (49°23.1'N, 124°13.5'W) and Station 43 (49°15.0'N, 123°39.4'W) near the BOMIS I site in May 1968 and April 1969, respectively. The relative locations of these stations are shown in Figure 15. The length of these records allowed a 29-day harmonic analysis to determine the tidal constants at 250m at Station 32 (see Data Record 1968-1969[10]) and at 300m at Station 43 (see Data Record 1969-1972[11]). Tables 9 and 10 list these tidal constants for the eight major current constituents at Station 32 and 43, respectively.

Predictions based upon these constants may be computed for any time, t, along the major axis with the following formula (Schuremen's manual[12])

$$U(t) = Uo + \sum_{i=1}^{8} N_i A_i \cos\left(F_i t + \left(V_o + U\right)_i - K_i^1\right) \qquad (1)$$

where

$U(t)$ = predicted current (cm/sec) along the major axis at time t (in hours from 0000 LST 1 January of prediction year)

U_o = mean velocity along the orthogonal axis.

N_i = node factor of ith constituent (Table 11).

A_i = harmonic amplitude (cm/sec) of ith constituent. (Listed in Tables 9 and 10 for Stations 32 and 43 respectively.)

F_i = speed (degrees/solar hour) of ith constituent (Table 12).

t = time (hours) measured from 0000 LST 1 January for prediction year.

---

[10] *Data Record of Current Observations, Strait of Georgia Section 3, Northwest Bay to McNaughton Point, 1968-1969,* Marine Sciences Directorate, Pacific Region, Victoria, BC, May 1, 1973

[11] *Data Record of Current Observations, Strait of Georgia Section 4, Gabriola Island to Gower Point, 1969-1972,* Marine Sciences Directorate, Pacific Region, Victoria, BC, October 1972

[12] *Manual of Harmonic Analysis and Prediction of Tides,* Paul Schuremen, U.S. Department of Commerce Special Publication No. 98, reprinted July 1976

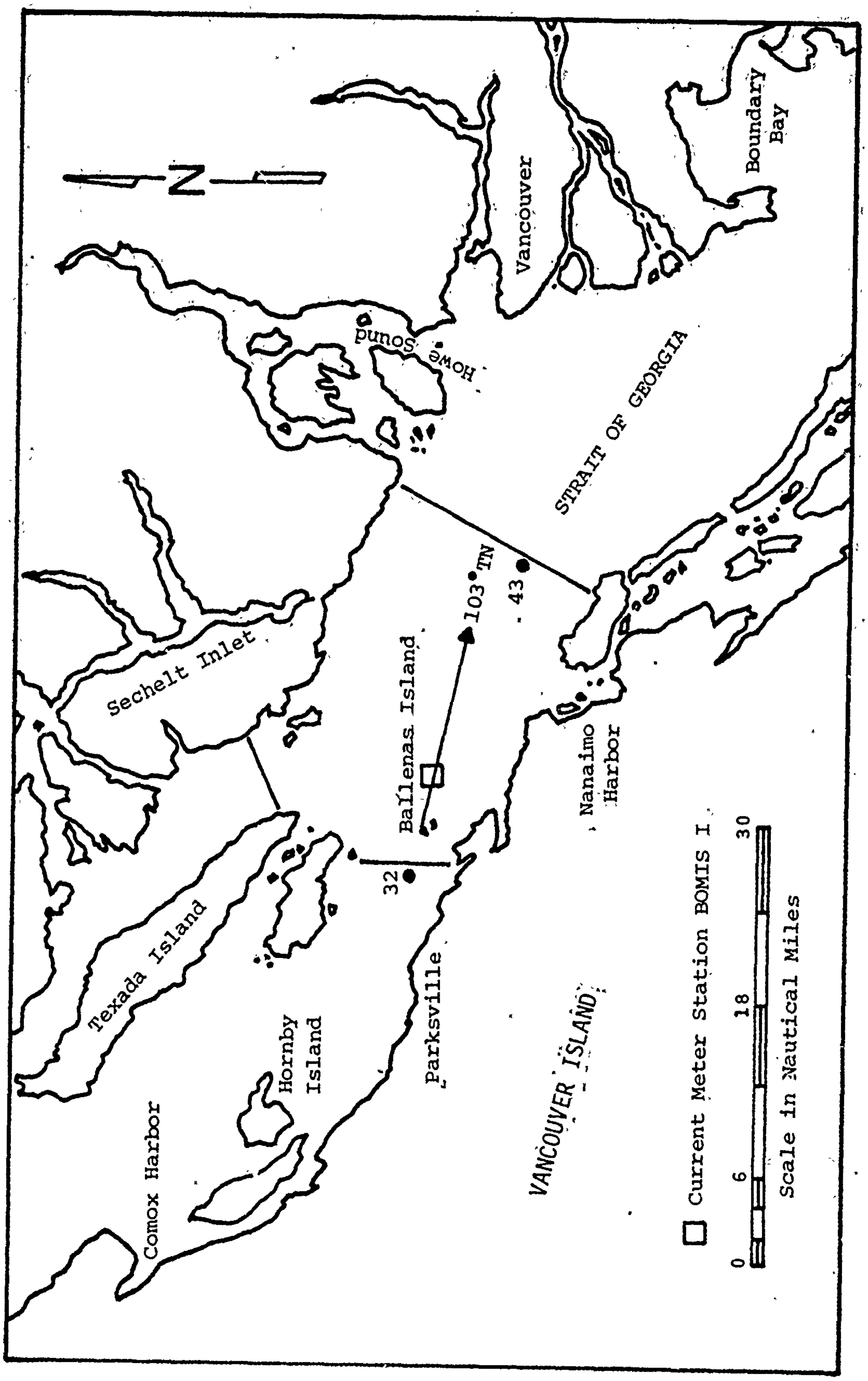

Figure 15. *Location of BOMIS I with Respect to Stations 32 and 43*

Table 9. Harmonic Constants (A & K^1)
for Station 32 (250m Depth)
(taken from reference 10)

Tidal Current Constituent	Major Axis A (cm/sec)	Major Axis K^1 (°)	Major Axis Ø (°TN)	Minor Axis A (cm/sec)	Minor Axis K^1 (°)	Minor Axis Ø (°TN)
K_1	3.8687	101.23	295	4.5338	275.34	25
O_1	1.7297	71.24	↓	2.5961	258.56	↓
P_1	1.2417	101.23	↓	1.4553	275.34	↓
M_2	4.0108	76.61	↓	3.7446	253.63	↓
S_2	1.1593	134.38	↓	1.6808	301.48	↓
K_2	0.3156	134.38	↓	0.4571	301.48	↓
N_2	0.8221	53.61	↓	0.7676	230.63	↓
M_4	0.5941	102.07	↓	0.6054	299.54	↓

Table 10. Harmonic Constants (A & K^1)
for Station 43 (300m Depth)
(taken from reference 11)

Tidal Current Constituent	Major Axis A (cm/sec)	Major Axis K^1 (°)	Major Axis Ø (°TN)	Minor Axis A (cm/sec)	Minor Axis K^1 (°)	Minor Axis Ø (°TN)
K_1	5.3405	86.39	295	1.4610	287.68	25
O_1	2.5477	81.82	↓	0.7022	287.06	↓
P_1	1.7143	86.39	↓	0.4690	287.68	↓
M_2	4.6697	79.77	↓	2.2013	267.49	↓
S_2	0.9575	97.34	↓	1.5701	302.55	↓
K_2	0.2605	97.34	↓	0.4273	302.55	↓
N_2	1.2978	4.4	↓	0.7145	179.17	↓
M_4	0.3295	180.99	↓	0.2481	45.35	↓

Table 11. Node Factor N_f for Middle of Each Year, 1970 to 1999 --from reference 12

Constituent	1970	1971	1972	1973	1974	1975	1976	1977	1978	1979
J_1	1.155	1.132	1.097	1.051	0.995	0.936	0.881	0.842	0.827	0.850
K_1	1.105	1.083	1.063	1.029	0.991	0.951	0.916	0.891	0.882	0.890
K_2	1.259	1.232	1.159	1.055	0.957	0.871	0.804	0.763	0.745	0.766
L_2	0.832	0.668	1.113	1.270	1.014	0.808	0.935	1.179	1.159	0.991
M_1	1.987	2.176	1.503	1.012	1.535	1.777	1.428	0.870	0.874	1.361
M_2*, N_2, 2N, λ_2, μ_2, ν_2	0.966	0.973	0.983	0.995	1.008	1.020	1.029	1.035	1.038	1.036
M_3	0.950	0.960	0.975	0.993	1.012	1.029	1.044	1.054	1.057	1.054
M_4, MN	0.934	0.948	0.967	0.991	1.016	1.039	1.059	1.072	1.077	1.073
M_6	0.903	0.922	0.951	0.986	1.024	1.060	1.090	1.110	1.118	1.112
M_8	0.873	0.898	0.935	0.981	1.032	1.081	1.122	1.149	1.160	1.151
O_1, Q_1, 2Q, ρ_1	1.170	1.143	1.101	1.047	0.984	0.920	0.863	0.822	0.806	0.819
OO	1.716	1.575	1.380	1.159	0.940	0.750	0.607	0.517	0.483	0.512
MK	1.068	1.059	1.045	1.024	0.998	0.970	0.943	0.923	0.915	0.922
2MK	1.032	1.031	1.023	1.020	1.006	0.989	0.970	0.956	0.950	0.955
Mf	1.417	1.341	1.233	1.102	0.962	0.831	0.723	0.652	0.625	0.647
Mm	0.882	0.903	0.940	0.982	1.025	1.067	1.100	1.123	1.131	1.121

Constituent	1980	1981	1982	1983	1984	1985	1986	1987	1988	1989
J_1	0.877	0.930	0.989	1.045	1.093	1.130	1.153	1.164	1.163	1.148
K_1	0.913	0.948	0.987	1.026	1.060	1.088	1.104	1.112	1.111	1.100
K_2	0.799	0.864	0.949	1.045	1.142	1.226	1.285	1.315	1.310	1.270
L_2	0.848	1.001	1.238	1.137	0.745	0.811	1.263	1.241	0.749	0.740
M_1	1.656	1.468	0.974	1.323	2.050	2.032	1.292	1.367	2.112	2.122
M_2*, N_2, 2N, λ_2, μ_2, ν_2	1.030	1.021	1.009	0.997	0.984	0.974	0.967	0.964	0.964	0.969
M_3	1.045	1.031	1.013	0.994	0.977	0.962	0.951	0.946	0.947	0.954
M_4, MN	1.061	1.042	1.018	0.993	0.969	0.949	0.935	0.928	0.930	0.939
M_6	1.092	1.063	1.027	0.989	0.954	0.924	0.904	0.894	0.896	0.910
M_8	1.125	1.085	1.036	0.986	0.939	0.901	0.874	0.862	0.864	0.881
O_1, Q_1, 2Q, ρ_1	0.858	0.915	0.979	1.041	1.096	1.140	1.168	1.182	1.180	1.161
OO	0.506	0.735	0.921	1.137	1.361	1.560	1.706	1.778	1.765	1.683
MK	0.941	0.967	0.996	1.022	1.043	1.058	1.068	1.072	1.071	1.065
2MK	0.969	0.987	1.005	1.019	1.027	1.031	1.032	1.032	1.032	1.032
Mf	0.715	0.820	0.949	1.088	1.221	1.333	1.412	1.450	1.443	1.392
Mm	1.103	1.070	1.029	0.986	0.944	0.909	0.884	0.872	0.874	0.891

Constituent	1990	1991	1992	1993	1994	1995	1996	1997	1998	1999
J_1	1.120	1.080	1.030	0.972	0.914	0.864	0.833	0.829	0.852	0.896
K_1	1.079	1.051	1.015	0.976	0.937	0.905	0.886	0.883	0.897	0.925
K_2	1.203	1.115	1.010	0.922	0.842	0.785	0.754	0.750	0.772	0.821
L_2	1.216	1.248	0.898	0.801	1.077	1.265	1.107	0.921	0.893	1.096
M_1	1.334	1.156	1.778	1.820	1.282	0.800	1.083	1.457	1.500	1.214
M_2*, N_2, 2N, λ_2, μ_2, ν_2	0.977	0.988	1.000	1.013	1.024	1.032	1.037	1.038	1.034	1.027
M_3	0.966	0.982	1.000	1.019	1.036	1.048	1.055	1.057	1.051	1.040
M_4, MN	0.955	0.976	1.000	1.025	1.048	1.065	1.075	1.076	1.069	1.054
M_6	0.932	0.964	1.000	1.038	1.072	1.099	1.115	1.117	1.105	1.082
M_8	0.911	0.952	1.000	1.051	1.098	1.134	1.156	1.159	1.143	1.111
O_1, Q_1, 2Q, ρ_1	1.128	1.081	1.024	0.960	0.897	0.844	0.812	0.808	0.832	0.879
OO	1.505	1.296	1.072	0.863	0.688	0.565	0.498	0.489	0.538	0.643
MK	1.054	1.038	1.015	0.988	0.959	0.934	0.918	0.916	0.928	0.950
2MK	1.030	1.025	1.015	1.000	0.982	0.964	0.952	0.951	0.959	0.976
Mf	1.303	1.184	1.048	0.910	0.786	0.691	0.636	0.629	[illegible]	0.752
Mm	0.918	0.956	0.993	1.042	1.081	1.110	1.128	1.130	[illegible]	1.091

* Factor f of MS, 2SM, and MSf are each equal to factor f of M_2.
Factor f of P_1, R_2, S_1, S_2, S_4, S_6, T_2, Sa, and Ssa are each unity.

BEST AVAILABLE COPY

Table 12. Constituent Speeds (F_i)

Harmonic Constituent	Speed (°/Solar Hour)
K_1	15.04107
O_1	13.94303
P_1	14.95893
M_2	28.98410
S_2	30.00000
K_2	30.08214
N_2	28.43973
M_4	57.96821

$(V_o+U)_i$ = equilibrium argument of ith constituent for prediction year (Table 13).

K_i^1 = local epoch of ith constituent (listed in Tables 9 and 10 for Stations 32 and 43 respectively.

A similar equation for the minor axis velocity may be obtained by substituting the minor axis mean velocity, the constituent amplitudes, and the local epochs for the minor axis values. Time series of predicted currents can then be computed.

The velocity vectors of the above-computed time series (major axis = 295°TN and minor axis = 025°TN) were transformed to coincide with the range-coordinate-system-resolved BOMIS I currents and thus provide the direct comparisons shown in Figures 16 and 17.

Figures 16 and 17 show the time series of the predicted currents at Station 32 (heavy line) and the measured currents at BOMIS I (light line) for the along-range and cross-range components, respectively. Time series of the differences between the measured currents at BOMIS I and the predicted currents at Station 32 are shown at the bottom of Figures 16 and 17. The average absolute differences in the along-range and cross-range components are 3.3 cm/sec and 3.4 cm/sec, respectively; however, there are numerous instances when the difference exceeds 10 cm/sec. The standard deviations of the along-range and cross-range differences are 4.1 cm/sec and 4.1 cm/sec, respectively.

Although not shown, comparison between the predicted currents at Station 43 and the measured currents at BOMIS I were generally similar. The along-range and cross-range standard deviation of

Table 13. Equilibrium Argument (V_0+U) for Meridian of Greenwich at Beginning of Each Calendar Year, 1970 to 1989 --from reference 12

Constituent	1970	1971	1972	1973	1974	1975	1976	1977	1978	1979
	°	°	°	°	°	°	°	°	°	°
J_1	270.0	1.8	93.1	197.4	256.0	11.3	100.2	195.6	281.3	4.9
K_1	13.4	15.5	17.1	19.0	19.2	18.2	16.2	14.1	10.5	6.8
K_2	207.2	211.5	211.8	218.4	218.2	215.8	211.5	207.6	200.9	191.2
L_2	262.8	60.3	215.2	81.8	282.4	99.0	276.4	99.7	297.9	130.9
M_1	155.2	48.0	307.8	231.9	158.7	51.8	302.5	198.6	135.7	41.8
M_2	165.4	260.8	8.0	81.5	185.3	256.5	26.0	101.8	201.8	301.9
M_3	68.1	40.2	11.9	300.8	277.0	218.0	219.0	152.7	122.7	92.8
M_4	330.0	173.6	15.9	169.1	10.5	211.5	52.1	203.6	11.7	211.8
M_6	136.3	80.1	23.9	253.6	195.8	137.2	78.1	305.3	215.5	185.7
M_8	301.7	347.1	31.8	318.2	21.0	63.0	101.1	47.1	87.3	127.5
N_2	270.1	282.7	295.2	270.0	282.0	293.8	305.3	279.3	290.6	301.9
2N	14.8	298.7	222.4	95.4	18.7	301.8	221.6	96.8	19.4	302.0
O_1	150.7	219.0	317.8	61.7	162.0	263.5	6.5	85.7	191.3	296.9
OO	58.7	326.4	234.6	163.0	61.0	321.1	212.6	125.5	9.8	253.0
P_1	349.8	350.0	350.2	349.5	349.7	350.0	350.2	349.5	349.7	349.9
Q_1	255.4	265.0	275.0	247.2	258.7	271.5	285.8	263.2	250.1	297.0
2Q	0.1	281.0	202.2	72.6	355.4	279.5	205.1	80.7	8.8	297.0
R_2	177.8	177.6	177.3	178.0	177.8	177.5	177.3	178.9	177.7	177.5
S_1	180.0	180.0	180.0	180.0	180.0	180.0	180.0	180.0	180.0	180.0
$S_2, 4, 6$	0.0	0.0	0.0	0.0	0.0	0.0	0.0	0.0	0.0	0.0
T_2	2.2	2.4	2.7	2.0	2.2	2.5	2.7	2.0	2.3	2.5
λ_2	285.6	197.4	109.1	7.6	278.8	189.8	100.6	358.2	268.8	179.4
μ_2	330.0	172.1	14.0	167.0	8.1	209.7	50.7	202.8	43.6	241.4
ν_2	225.3	156.1	86.8	311.5	271.7	201.7	131.4	25.3	311.0	211.1
ρ_1	210.6	128.1	66.6	313.7	218.1	179.1	111.9	9.2	301.3	239.4
MK	178.0	282.3	25.1	105.6	201.4	301.0	42.2	115.9	312.5	208.7
2MK	317.4	158.1	358.8	150.0	351.1	193.3	35.9	169.4	33.2	287.0
MN	75.0	189.5	303.2	351.5	107.2	219.5	331.3	21.1	132.9	241.8
MS	165.4	250.8	3.0	81.5	185.3	255.8	26.0	101.8	201.8	301.9
2SM	191.6	93.2	352.0	275.5	171.7	71.2	334.0	258.2	158.2	58.1
Mf	44.0	308.7	212.4	111.1	41.3	298.8	193.0	110.4	350.3	218.0
MSf	191.6	93.2	352.0	275.5	171.7	71.2	334.0	258.2	158.2	58.1
Mm	255.3	314.0	72.8	171.6	263.3	352.0	50.7	182.5	271.2	0.0
Sa	280.2	280.0	279.8	280.5	280.3	280.0	279.8	280.6	280.3	280.1
Ssa	200.5	200.0	199.5	201.0	200.5	200.0	199.6	201.1	200.6	200.1

Constituent	1980	1981	1982	1983	1984	1985	1986	1987	1988	1989
	°	°	°	°	°	°	°	°	°	°
J_1	89.1	188.9	276.5	5.6	95.8	201.0	292.7	21.7	110.8	222.8
K_1	3.7	2.5	1.5	1.5	2.4	1.9	6.0	9.2	11.6	14.8
K_2	188.2	185.6	183.1	182.6	184.2	189.3	191.5	196.3	203.3	210.0
L_2	310.2	116.6	313.4	159.2	350.3	135.8	341.5	188.0	25.5	160.0
M_1	291.5	170.8	87.9	30.0	291.6	171.7	32.0	31.2	290.1	170.8
M_2	42.0	117.0	218.4	319.1	60.0	136.8	236.1	330.6	81.0	158.1
M_3	63.0	356.8	327.6	298.6	270.0	205.2	177.2	149.3	121.6	57.1
M_4	84.0	235.8	76.7	278.1	120.0	273.6	116.2	319.1	162.1	316.2
M_6	126.0	353.7	295.1	237.2	180.0	50.3	251.3	298.7	213.1	111.2
M_8	168.0	111.6	153.4	196.2	210.0	187.1	232.4	278.2	324.1	272.3
N_2	313.3	287.4	299.2	311.2	323.4	298.4	311.0	323.7	336.4	311.7
2N	224.7	97.0	20.0	303.2	226.7	100.0	21.8	307.8	231.0	105.3
O_1	41.6	119.4	221.1	321.1	60.8	131.2	232.6	330.7	68.8	111.6
OO	139.2	57.5	313.6	213.9	117.6	51.0	316.5	227.0	135.6	71.2
P_1	350.2	349.4	349.7	349.9	350.2	349.4	349.6	349.9	350.1	349.8
Q_1	312.9	289.0	301.9	311.5	321.2	295.8	305.4	314.8	321.2	285.8
2Q	221.3	98.5	22.7	305.6	227.5	97.4	18.3	290.0	219.2	89.0
R_2	177.2	178.0	177.7	177.4	177.2	177.9	177.7	177.4	177.2	177.9
S_1	180.0	180.0	180.0	180.0	180.0	180.0	180.0	180.0	180.0	180.0
$S_2, 4, 6$	0.0	0.0	0.0	0.0	0.0	0.0	0.0	0.0	0.0	0.0
T_2	2.8	2.0	2.3	2.6	2.8	2.1	2.3	2.6	2.8	2.1
λ_2	90.0	317.8	258.8	170.0	81.4	310.0	251.9	163.0	75.0	331.8
μ_2	55.3	237.6	78.8	280.2	121.0	275.1	117.2	310.1	161.6	316.0
ν_2	171.0	68.0	358.0	298.2	218.6	113.5	44.3	346.2	266.2	161.4
ρ_1	173.6	69.6	0.7	290.5	219.4	110.9	38.8	326.4	274.0	115.0
MK	45.7	120.4	219.8	320.5	62.4	141.7	245.0	348.8	92.6	172.8
2MK	80.1	233.3	75.3	276.6	117.6	268.6	109.3	309.9	151.5	301.4
MN	355.3	15.3	157.5	212.2	23.4	76.1	189.1	303.2	57.5	100.8
MS	42.0	117.0	218.4	319.1	60.0	136.8	236.1	330.6	81.0	158.1
2SM	318.0	212.1	111.6	40.9	300.0	223.2	121.9	20.4	270.0	201.9
Mf	138.8	59.0	316.2	216.2	118.4	48.4	313.0	228.1	123.4	54.8
MSf	318.0	212.1	141.6	40.9	300.0	223.2	121.9	20.4	270.0	201.9
Mm	88.7	190.5	279.2	7.6	96.6	108.4	287.1	15.9	101.6	206.4
Sa	279.8	280.6	280.3	280.1	279.8	280.6	280.4	280.1	279.9	280.6
Ssa	199.6	201.1	200.6	200.2	199.7	201.2	200.7	200.2	199.8	201.3

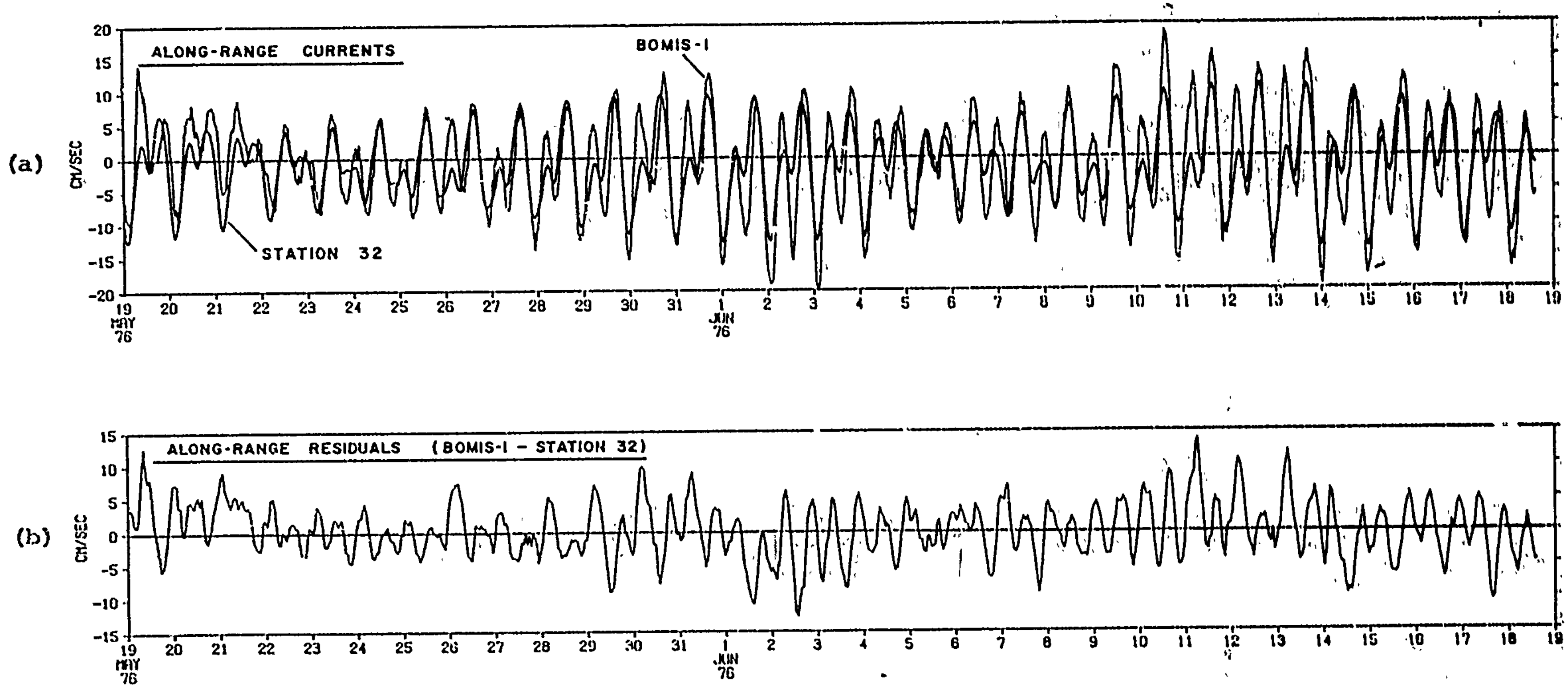

Figure 16. Along-Range Currents
(a) Predicted (Station 32) versus Measured (BOMIS I)
(b) Difference (Residual, BOMIS I minus Station 32)

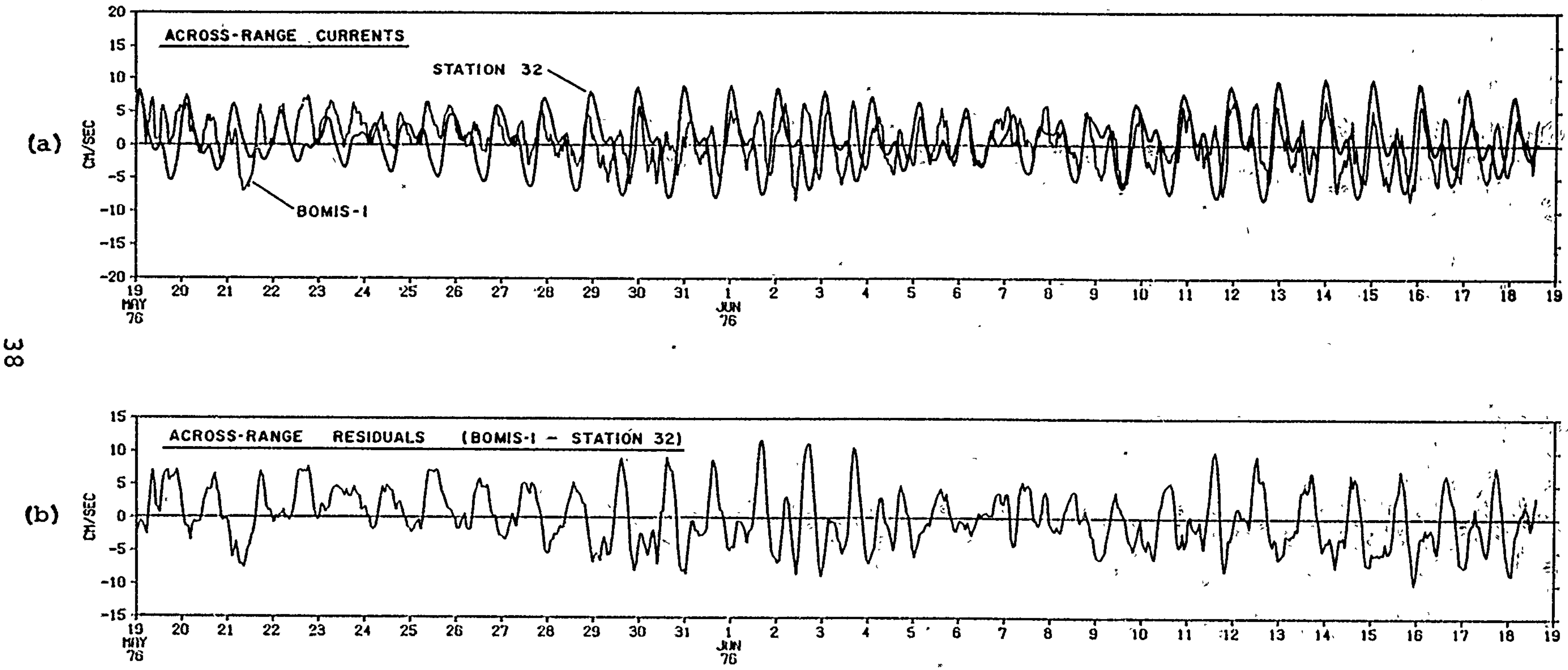

Figure 17. Cross-Range Currents
(a) Predicted (Station 32) versus Measured (BOMIS I)
(b) Difference (Residual, BOMIS I minus Station 32)

these differences were 4.4 cm/sec and 3.0 cm/sec, respectively. The lag-correlation function (top) and scatter diagram (bottom) between the along-range currents measured at 274m depth at the BOMIS I site and at 250m depth at Station 32 are shown in Figure 18.

Linear regression equations relating the above time series and the standard deviations, σ,* about these regressions were computed:

Along range:

$$U_{\text{BOMIS I}} = 0.3 + 1.037\ U_{\text{Station 32}};\ \sigma = 4.1 \text{ cm/sec} \quad (2)$$

$$U_{\text{BOMIS I}} = 1.5 + 0.895\ U_{\text{Station 43}};\ \sigma = 4.3 \text{ cm/sec} \quad (3)$$

Cross range:

$$V_{\text{BOMIS I}} = 0.5 + 0.337\ V_{\text{Station 32}};\ \sigma = 2.9 \text{ cm/sec} \quad (4)$$

$$V_{\text{BOMIS I}} = 1.2 + 1.003\ V_{\text{Station 43}};\ \sigma = 2.9 \text{ cm/sec} \quad (5)$$

The above standard deviations represent an estimate of the quality of this predictive method. Stations 32 and 43 are separated by 24 nautical miles and bracket the BOMIS I site. Based upon the above comparisons, horizontal variations in the prediction quality are small. The standard deviation about the along-range regression increased from 4.1 to 4.3 cm/sec with a doubling of distance from BOMIS I.

Examination of the difference between the predicted currents (see Figures 16 and 17) and the measured currents summarized in Figures 11, 12, 13, and 14 suggests that the residual signal contains a dominant tidal component. This may in part be due to variations in the baroclinic component of the tides.† See VonArx's *Introduction to Physical Oceanography*.[13]

The harmonic constant method of predicting the along-range and cross-range currents at 274m depth at the BOMIS I site involves the following steps:

**Computed from the difference series generated by subtracting predicted current from measured current.*

†*A baroclinic tide (motion) exists when constant pressure (isobaric) surfaces and constant density (isopycnal) surfaces intersect. A baroclinic fluid cannot remain motionless.*

[13]*Introduction to Physical Oceanography*, W. S. VonArx, Addison-Wesley Publishing Company, Inc. Reading, Massachusetts

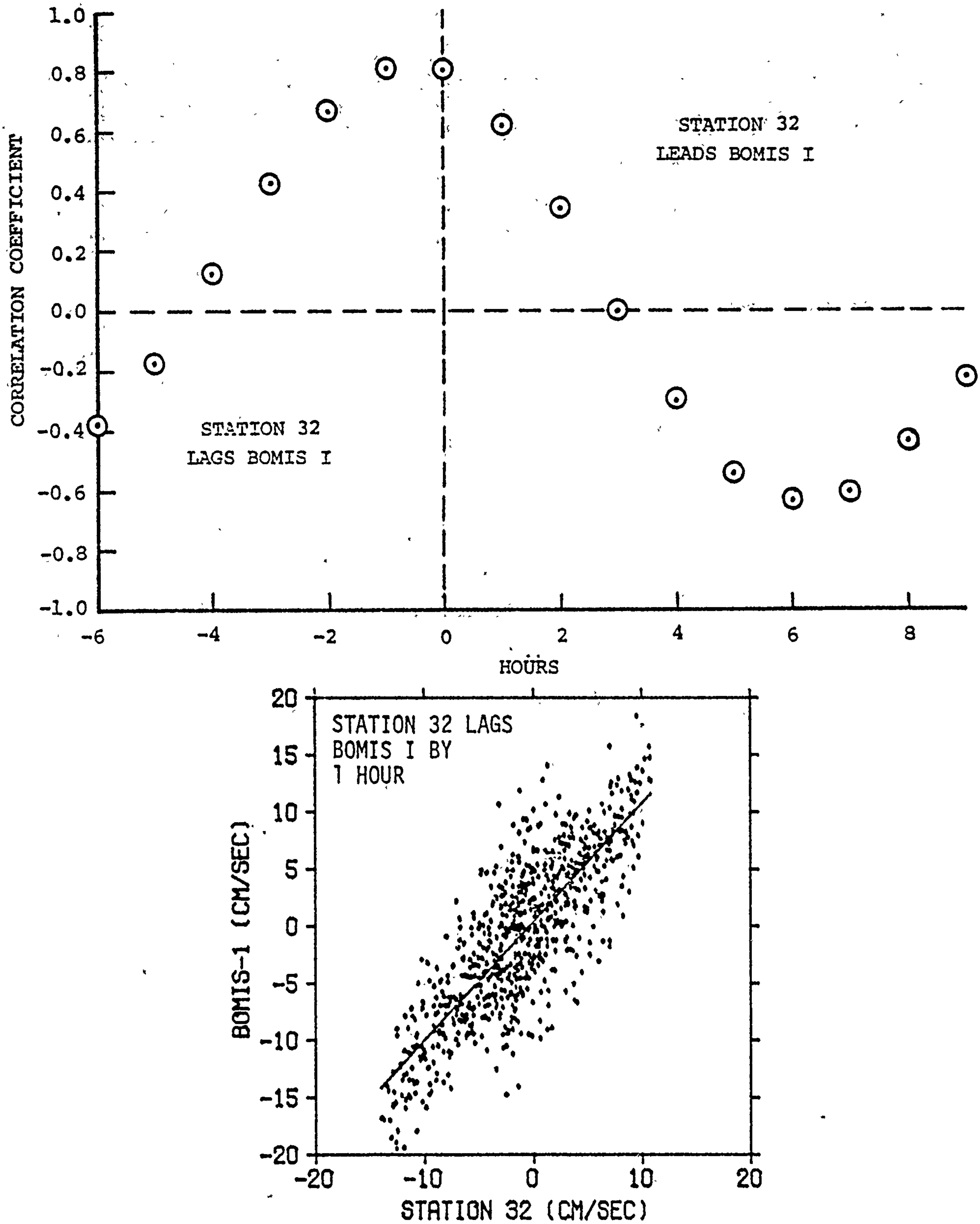

Figure 18. Lag Correlation Function (Top) and Scatter Diagram (Bottom) Between the Along-Range Current Measured at BOMIS I and the Station 32 Predicted Current

1. Compute future currents for Station 32 based upon published harmonic constants. Such time series may be tabulated with a desk computer. The program listing for an HP 9820 computer is provided in Appendix D.

2. Look up Station 32 one hour after the desired prediction time (1-hour lag).

3. Compute the along-range and cross-range current predictions for the 274m depth at the BOMIS I site using equations (2) and (4), respectively, with Station 32 predicted currents.

Based upon the recent 31-day measured currents at 274m depth at the BOMIS I site the along-range and cross-range predictions will be statistically within ±8.2 cm/sec and ±5.8 cm/sec (2σ), respectively, approximately 95 per cent of the time.

TIDAL HEIGHT CORRELATION METHOD

Tidal heights measured at nearby Winchelsea Island were correlated to the measured currents at the BOMIS I site and found to be useful for input to a prediction method. Time series of hourly tide heights during the period when the VACM was deployed were generated from data provided by Environment Canada. Unfortunately a 14-hour gap exists in these data, necessitating two sets of calculations using 16.7- and 13.3-day records.

The tides in the Strait of Georgia are of a mixed type with a predominant diurnal inequality. Both the diurnal and semidiurnal components behave as standing waves (see Refield's *Analysis of Tidal Phenomena in Narrow Embayments*[14] and Crean's Technical Report No. 156[15]) in which the tide heights are approximately 90° out of phase with the current velocities. The lag correlation functions were computed for these data sets, and the one using the 16.7-day tide record is shown in Figure 19. For both tide record segments the best correlation occurs when the tide heights lead the along-range current velocities by 4 hours. The scatter diagram with this 4-hour lead included is also shown in Figure 19. Linear regression equations relating tide height to current velocity at 274m and the standard deviations, σ, about these regressions are:

[14]*The Analysis of Tidal Phenomena in Narrow Embayments*, Alfred C. Redfield, Contribution No. 529 from the Woods Hole Oceanographic Institution and the Oceanographic Laboratories, University of Washington

[15]Technical Report No. 156, *A One-Dimensional Hydrodynamical Numerical Tidal Model of the Georgia-Juan de Fuca Strait System*, P. B. Crean, Fisheries Research Board of Canada, 1969

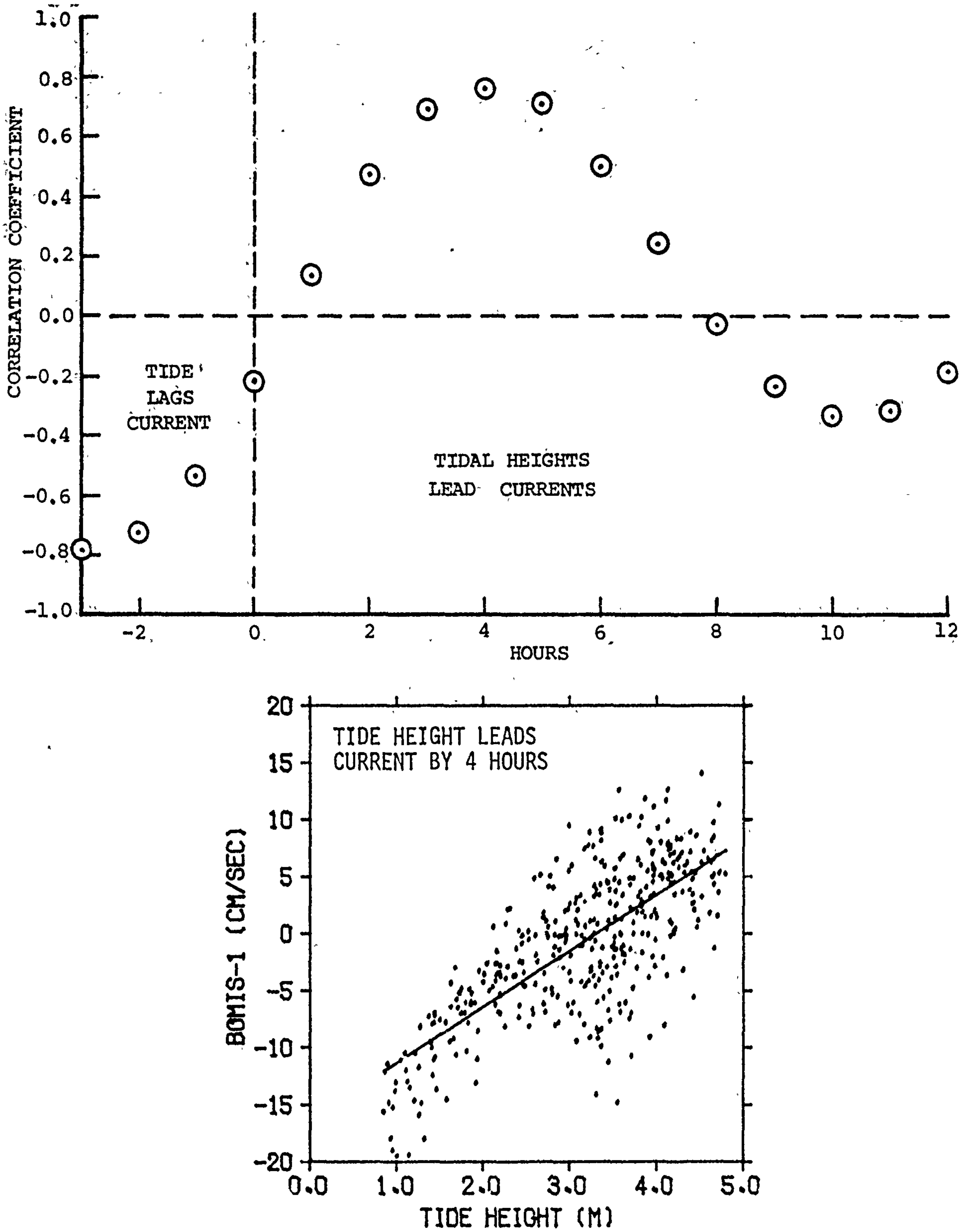

Figure 19. Lag Correlation Function (Top) and Scatter Diagram (Bottom) Between the Along-Range Current Measured at BOMIS I and the Winchelsea Island Tide Height (in meters)

Along-range (tide heights preceding test time by 4 hours)

$$U_{\text{BOMIS I}} = -16.2 + 4.885\ H_I;\ \sigma = 4.4\ \text{cm/sec} \quad (6)$$

Cross-range (tide heights preceding test time by 5 hours)

$$V_{\text{BOMIS I}} = 5.7 + 1.434\ H_I;\ \sigma = 2.7\ \text{cm/sec} \quad (7)$$

Comparisons using the shorter (13.3-day) tidal-height series produced coefficients with similar standard deviations (4.9 vs 4.4 cm/sec and 2.6 vs 2.7 cm/sec; see Table 14).

Thus the tidal height correlation method of predicting the along-range and cross-range currents at 274m at the BOMIS I site involves the following steps:

1. Read the tidal heights (in meters) 4 hours and 5 hours prior to the desired prediction time. For example, if a test is scheduled for 1200, utilize the tide height at 0800 and 0700 to predict along-range and cross-range currents respectively.

2. Compute the along-range and cross-range current predictions using equation (6) with the 4-hour preceding tide height value and equation (7) with the 5-hour preceding tide height value, respectively.

The along-range and cross-range predictions will be within ±8.8 cm/sec and ±5.4 cm/sec (2σ), respectively, approximately 95 per cent of the time.*

SUMMARY OF PREDICTION METHODS

The currents at 274m depth at the BOMIS I site are approximately normally distributed, 95 per cent of the along-range and cross-range velocities being within the ranges -15 to +12 and ±6 cm/sec, respectively (see Figures 12 and 14).

Since 78.5 per cent of the variance occurs at tidal frequencies, two simple prediction methods based upon tidally dominated input signals were examined: 1. harmonic constant method and 2. tidal height correlation method.

Table 14 summarizes the per cent of energy linearly correlated by the above methods and the standard deviations of the residual error. These methods account for 54 - 66 per cent of the along-range and 18 - 37 per cent of the cross-range energy.

The 95 per cent interval assumes that the residuals are normally distributed.

Table 14. Current Prediction Method Comparison[a]

	ALONG-RANGE		CROSS-RANGE		SPEED	
	% Energy (%)	Standard Deviation (cm/sec)	% Energy (%)	Standard Deviation (cm/sec)	% Energy (%)	Standard Deviation (cm/sec)
BOMIS I						
(Δt=30 minutes)	–	7.2	–	3.2	–	3.9
Non-Tidal	–	2.8	–	2.4[b]	–	–
HARMONIC CONSTANT METHOD						
Constants						
Station 32	66	4.1	18	2.9	37	3.0
Station 43	63	4.3	18	2.9	36	3.0
TIDAL HEIGHT CORRELATION METHOD						
Winchelsea Island						
16.7-day tidal record	54	4.4	22	2.7	16	3.3
13.3-day tidal record	60	4.9	37	2.6	12	3.7

[a] *Specifically, per cent energy that is linearly correlated by prediction methods described in text and standard deviations of the residuals about the regression equations. Also shown is the standard deviation of the 30-minute averaged basic data and the non-tidal component at 274m depth at the BOMIS I site.*

[b] *Computed value of σ is 2.36, which is rounded off to 2.4. (2σ = 4.7 as noted on page 25)*

The harmonic constant method, which explained the largest percentage of the along-range energy (66%) reduced the standard deviation of the residual signal to 4.1 cm/sec. (The standard deviation of the original along-range component was 7.2 cm/sec.) The tidal height correlation method, which explained the largest percentage of the cross-range energy (37%) reduced the standard deviation of the residual signal to 2.6 cm/sec when lagged 5 hours. (The standard deviation of the original cross-range component was 3.2 cm/sec.)

6. CONCLUSIONS

1. Enough valid data were acquired to statistically definitize the current characteristics at 274m depth. This definitization is provided in Tables 1 and 2.

2. The lower limit of the standard deviations of the residuals (i.e., non-tidal variations) of any tidally-based prediction scheme for Nanoose is presently estimated as 2.8 cm/sec for the along-range component and 2.4 cm/sec for the cross-range component.

3. Use of equations (2) and (7) is recommended for prediction of along-range and cross-range current velocities respectively. The 2σ confidence intervals associated with these equations are ±8.2 cm/sec along range and ±5.4 cm/sec cross range. The 2σ interval represents the 95 per cent confidence interval of normally distributed data.

4. Although the predictions using the above methods do not greatly reduce the variance of the residual or unknown signal, they do entail smaller standard deviations than can be predicted using measured current statistics alone (7.2 raw to 4.1 and 3.2 raw to 2.6, see Table 14).

5. A lower confidence interval for predicted currents, using equations (2) and (7), awaits further long-term current measurements (over a one-year period at least), concurrent with water stratification and meteorological studies to determine the causes and methods for predicting the low-frequency currents shown in Figure 10.

6. It is important to emphasize that the above discussion and predictive statistics are valid only for one depth at one location during one season. Little can accurately be said about the horizontal spatial variations or the seasonal temporal variations of the range currents. A qualitative feeling concerning current ranges and amplitude may be suggested for other locations, depths, and seasons, but nothing more.

7. RECOMMENDATIONS

1. If a quantitative resolution to present uncertainties in current prediction caused by lack of spatial and temporal (seasonal) data is required (because of these spatial and temporal uncertainties), it is recommended that the following be given further study:

a. Seasonal variations in range currents at one location. Field efforts should include deployment of current meters at one or more depths, measurement of the density field, and concurrent sampling of atmospheric pressure and wind stress, all for a full year. Information concerning variations in the low-frequency currents on a seasonal time scale as well as baroclinic variations in the tidal currents (due to seasonal density changes) may be gained.

b. Spatial variations in range currents over a 2-3 month period. Field efforts should include deployment of current meters at two or more locations. Horizontal variations in both the tidal and low-frequency components of currents should be studied.

2. Only a very cursory look at the vertical variation of currents has been taken so far. The above recommendations should include vertically separated current meter positioning whenever resources permit.

3. An examination of Dr. Pat Crean's (1969) numerical tidal model of the Strait of Georgia/Strait of Juan de Fuca/Puget Sound System should be pursued. Comparison of his predictions with measured currents should be made to determine if his model may provide greater accuracy than the simplistic methods described in this report.

4. Project engineers should review Tables 1, 2, and 4 for the uncertainties risked if current measurements are not made and should advise whether these risks are acceptable or if measurements should be made. If the measurements are needed, specific requirements should be stated so that cost can be estimated against probable benefit.

REFERENCES

1. Research & Engineering Department Memo 222-76, *Current Speeds at the Dabob Bay, Nanoose and BARSTUR Tracking Ranges and Effects on Mine Mark 60*, 11 May 1976

2. Paquette, R. G., *Practical Problems in the Direct Measurement of Ocean Currents*, Proceedings of the Symposium on Transducers for Oceanic Research, Marine Sciences Instrumentation, Vol. 2, Plenum Press, New York, 1963

3. *Vector Averaging Current Meter Model 610* manual, AMF Electrical Products Development Division, September 1973

4. NOAA-TM-NOS-NOIC-1, *Report on the Evaluation of a Vector Averaging Current Meter*, William E. Woodward and Gerald F. Appel, July 1973

5. NOAA-TM-NOS-NOIC-3, *Effects of Vertical Motion on Vector Averaging (Savonius Rotor) and Electromagnetic Type Current Meters*, A. N. Kalvaitis, March 1974

6. Deep-Sea Research 21, *An Intercomparison of Three Current Meters Operating in Shallow Water*, D. Halpern and others, pp 489-497, 1974

7. Deep-Sea Research 23, *Near Surface Current Measurements*, P. M. Saunders, pp 249-258, 1976

8. *The Analysis of Tides*, Gabriel Godin, University of Toronto Press, 1972

9. *VECPLOT: A Graphics Program to Display Current and Wind Time-Series Data*, J. R. Holbrook and D. Halpern, Proceedings of the Working Conference on Oceanographic Data Systems, Woods Hole Oceanographic Institution, pp 217-232, 1975

10. *Data Record of Current Observations, Strait of Georgia Section 3, Northwest Bay to McNaughton Point, 1968-1969*, Marine Sciences Directorate, Pacific Region, Victoria, BC, May 1, 1973

11. *Data Record of Current Observations, Strait of Georgia Section 4, Gabriola Island to Gower Point, 1969-1972*, Marine Sciences Directorate, Pacific Region, Victoria, BC, October 1972

12. *Manual of Harmonic Analysis and Prediction of Tides*, Paul Schuremen, U. S. Department of Commerce Special Publication No. 98, reprinted July 1976

--continued

REFERENCES --concluded

13. *Introduction to Physical Oceanography,* W. S. VonArx, Addison-Wesley Publishing Company, Inc. Reading, Massachusetts

14. *The Analysis of Tidal Phenomena in Narrow Embayments,* Alfred C. Redfield, Contribution No. 529 from the Woods Hole Oceanographic Institution and the Oceanographic Laboratories, University of Washington

15. Technical Report No. 156, *A One-Dimensional Hydrodynamical Numerical Tidal Model of the Georgia-Juan de Fuca Strait System,* P. B. Crean, Fisheries Research Board of Canada, 1969

ARTN 75-9

Appendix A

CURRENT STUDIES AT THE NANOOSE RANGE

by

Robert A. Helton

and

Kjar G. Willey

Applied Research Division
Research and Engineering Department
Naval Torpedo Station
Keyport, Washington 98345

1. Introduction

a. Current measurements have been conducted for several years at the NAVTORPSTA tracking ranges. The measurement apparatus entails a Hydro Products Savonius rotor and directional vane follower. These sensors are part of the presently utilized STVP systems which are employed aboard the range craft. The current speed and especially the sampled (once a minute) current direction are both subject to errors caused by pendulation and roll of the range craft during data acquisition (range craft is moored). Because of this problem and the prohibitive expense of deploying a range craft STVP system, it was proposed by the author to tether an appropriate self-contained current measuring instrument to BOMIS and acquire quality data for two purposes. Quality here refers to confidence in the indicated current direction.

b. The foremost purpose was to measure current profiles (speed and direction versus depth) and stratum tidal currents while tracking the BOMIS buoy. This will allow the determination of horizontal offset distance and dynamics in characteristic current field structures when BOMIS is raised and lowered. Positional data have been analyzed and will be compared to the results predicted by the Kelf (Code 7022) tethered buoy drag model.

It was initially felt that the BOMIS buoy would suffer little motion in the expected current structure at Nanoose. Such has turned out to be the case as BOMIS offsets were minimal and the equilibrium position was reached quickly (less than 4 minutes) during the raising and lowering processes. Another separate report on BOMIS offset and dynamics is in progress.

c. The secondary purpose was to investigate the current structure and the transport of cells entailing temperature discontinuities. Tidal currents assume importance when considering offset of ordnance devices during ballistic tests. Cells become important when their occurence causes refractive anomalies due to temporal discontinuities produced in the sound speed structure.

d. This technical note will discuss the current data acquired by tethering an American Machine and Foundary (AMF) Vector Averaging Current Meter (VACM) atop the BOMIS buoy for 37.2 days. A VACM is a commercially available state-of-the-art instrument. It accurately measures current speed, direction and water temperature and internally records these parameters along with accurate elapsed time so measurement depth variations can be correlated with the recorded data. Data are sampled every 1/8 turn of the rotor. In a current speed of 1 knot, approximately 11 samples/second are acquired for internal vector averaging. References 1, 2, and 3 discuss the attributes, accuracy limitations and theory of operation of the VACM respectively.

2. Measurement Planning and Execution

a. Contact was established with Dr. David Halpern of the now Pacific Marine Environmental Laboratory in February 1974 concerning current measurement techniques. Halpern quickly endorsed the idea of making multi-depth current observations and acquiring current profile data by using a single current meter positioned in hydrospace by BOMIS. A joint experiment was developed. Halpern and his staff enthusiastically prepared and loaned a VACM for the measurement period. After returning the instrument, the data tape was processed and plots, tabular data, etc. were all furnished gratis in exchange for joint data usage.

b. The VACM deployment, retrieval, etc. and the run plan preparation (RP 9125), execution, BOMIS positioning coordination, etc. were managed by M. Kelf and K. Willey respectively. Mr. Willey also correlated the BOMIS operation log book times with the internally recorded VACM time to identify the current profile and the constant depth data periods. The VACM was tethered to the BOMIS buoy on 29 March 1975 and retrieved on 5 May. BOMIS I was then positioned at X = 10,213 yards and Y = -243 yards. The positional relationship of the VACM to the Winchelsea Island (WI) tide gage is shown in Figure 1. Tide data were provided by Mr. W. J. Rapatz, A/Regional Tidal Supervisor of the Institute of Ocean Sciences, Pacific Region.

3. Data Reduction

Two data tabs and several computer generated plots were provided by Halpern, et al. One tab lists the acquired data for each 56.25-second sampling time interval. The other tab averages 16 of the samples to yield a 15-minute data average. Some of the computer generated plots are provided as Figures 2 through 5 in this report.

By comparing the record of tidal height at WI with the record of current speed and direction, the characterization of tidal currents can be deduced. It should be noted that the magnetic north referenced current directions were "computer rotated" so the +Y range axis becomes 0 degrees or the data reference. A current direction of 43° is therefore actually 56°TN.

4. Data Analysis

a. Profile Data.

The VACM was raised or lowered to various depths with generally 15 minutes of residence time allowed at each depth. This permitted the buoy to attain its maximum excursion, settle down, etc. and still allowed approximately 10 minutes of stable platform data acquisition. Because the profile was temporally acquired, some distortion must exist in the profile data due to some variation in the tidal stage. Table 1 lists the averaged stratum level currents and directions obtained at the indicated depths for each of seven current profiling depth excursions. A current strength of 23.5 cm/sec in a direction of 107° at 15.2-meter depth is indicated as 107°/23.5 in Table 1.

Table 2 further summarizes the profile values of Table 1 into observed ranges for the current direction and strength observed at selected depths under various stages of ebb and flood tide.

b. Constant Depth Data.

Data averaged over a 15-minute time interval (average of sixteen 56.25-second interval data samples) were examined to determine the range of the current speed and direction. This analysis is summarized in Table 3. With few exceptions, depth wise, the current waned to zero for many time periods in the 1- to 10-minute range and longer. Histograms for current speed and direction for all the data are shown in Figures 2 and 3 respectively.

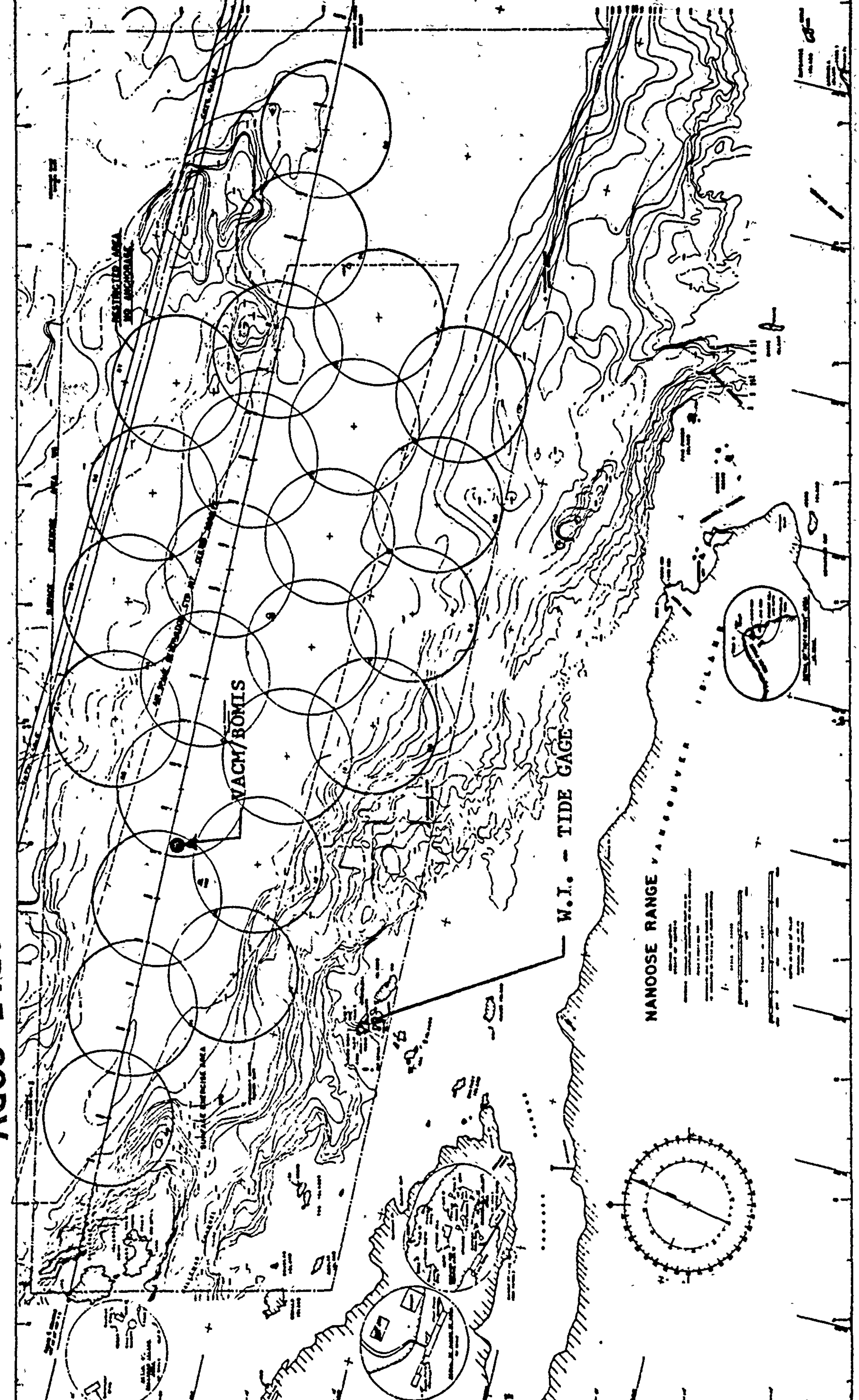

Figure 1. Position of VACM

TABLE 1. CURRENT PROFILE DATA (56.25 sec sample periods)

Depth	EBB TIDE				FLOOD TIDE			
Meters	31 March "up"	11 April "down"	11 April "up"	29 April "down"	7 April "up"	11 April "up"	24 April "down"	
~ 15.2	107°/23.5	78°/26.8		168°/10.2	28°/10.5	113°/10.7	30°/15.1	
30.5	103°/19.4	84°/28.8		82°/18.7	78°/ 7.5	29°/11.6	260°/ 8.0	
45.7								
61.0	74°/23.7	82°/18.6		104°/11.2	103°/ 1.8	111°/13.2	299°/ 7.5	
91.4	98°/20.2	106°/ 9.6		108°/13.4	339°/ 1.8	119°/ 9.1	300°/ 4.2	
121.9	116°/ 6.8	157°/ 8.8		146°/12.4	275°/ 4.7	165°/ 5.7	217°/10.3	
152.4	11°/ 9.1	177°/12.0		93°/ 6.0	257°/ 8.4	241°/ 8.2	244°/11.6	
182.9		172°/12.7		83°/ 5.5	284°/ 8.5	255°/16.9	279°/10.7	
213.4		181°/ 4.3				219°/16.5		
243.8	94°/ 9.0	133°/ 4.5	56°/1.8	73°/ 3.4	302°/ 6.3	219°/11.4	279°/14.1	
274.3		92°/ 5.4	73°/6.0	74°/ 4.5		248°/ 7.5		
304.8		101°/ 6.5	93°/7.3			237°/ 4.4		
335.3		67°/ 4.6	76°/6.3	50°/ 6.5		86°/ 1.7		
365.8	355°/ 3.5	64°/ 8.2	56°/7.0	49°/ 5.1	235°/ 9.7		250°/10.0	
396.2		64°/ 6.7	53°/7.1	60°/ 4.7		118°/ 4.1		
~411.5				67°/ 7.1		64°/ 7.8		

TABLE 2. RANGE OF CURRENT SPEEDS AND DIRECTIONS (PROFILE DATA)

Depth	EBB TIDE		FLOOD TIDE	
Meters	Direction Degrees	Speed cm/sec	Direction Degrees	Speed cm/sec
∿ 15.2	78-168	10.2-26.8	28-113	10.5-15.1
30.5	82-103	18.7-28.8	29-260	7.5-11.6
45.7				
61.0	74-104	11.2-23.7	103-299	1.8-13.2
91.4	98-108	9.6-20.2	119-339	1.8-9.1
121.9	116-157	6.8-12.4	165-275	4.7-10.3
152.4	11-177	6.0-12.0	241-257	8.2-11.6
182.9	83-172	5.5-12.7	225-284	8.5-16.9
213.4	181	4.3	219	16.5
243.8	56-133	1.8-9.0	219-302	6.3-14.1
274.3	74-92	4.5-6.0	248	7.5
304.8	93-101	6.5-7.3	237	4.4
335.3	50-76	4.6-6.5	86	1.7
365.8	355-64	3.5-8.2	235-250	9.7-10.0
396.2	53-64	4.7-7.1	118	4.1
∿411.5	67	7.1	64	7.8

TABLE 3. RANGE OF CONSTANT DEPTH DATA (15 minute data average)

Depth Meters	Date/Time Span	Direction Degrees	Speed cm/sec
61.0	7 April:1400→ 9 April:0900	335→132	0.0→21.0
61.0	9 April:1600→10 April:0900	28→153	0.0→18.2
61.0	10 April:1715→11 April:0730	62→113	4.0→15.1
91.4	15 April:1000→18 April:0900	42→356	0.0→11.7
91.4	25 April:1400→28 April:1245	3→354	0.0→28.5
121.9	4 April:1245→ 7 April:0945	1→359	0.0→20.7
152.4	29 March:1600→31 March:0900	270→359	8.2→38.0
182.9	11 April:1500→14 April:0845	32→9	0.0→22.3
213.4	14 April:1230→15 April:0830	238→321	0.0→20.7
274.32	2 May :1200→ 5 May :1100	19→294	0.0→13.3
365.8	18 April:1100→21 April:0730	31→265	0.0→15.3

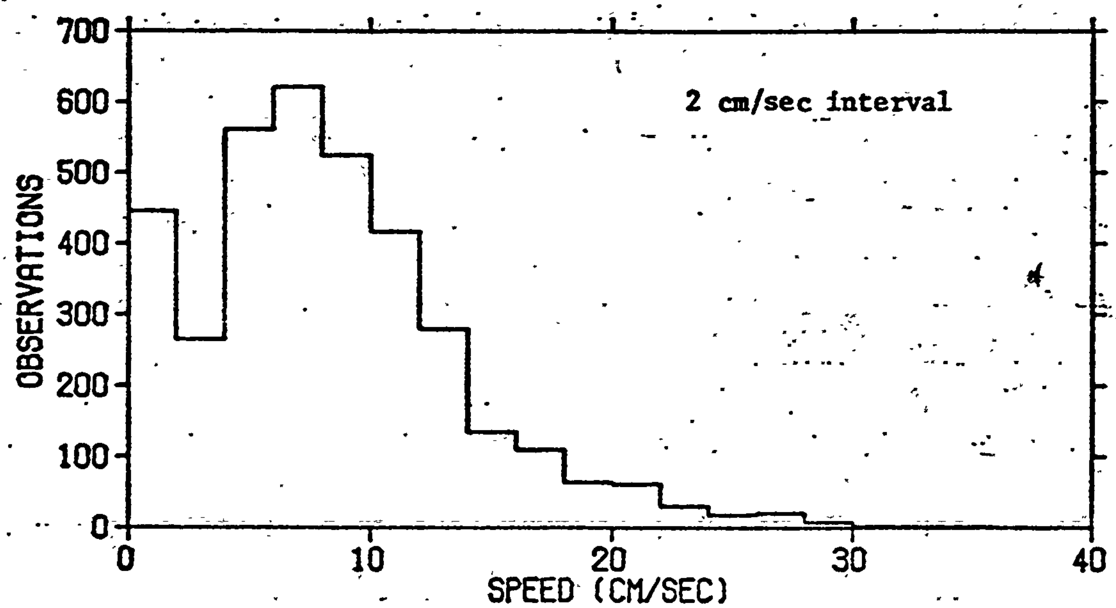

Figure 2. Current Speed Distribution (all data and all depths).

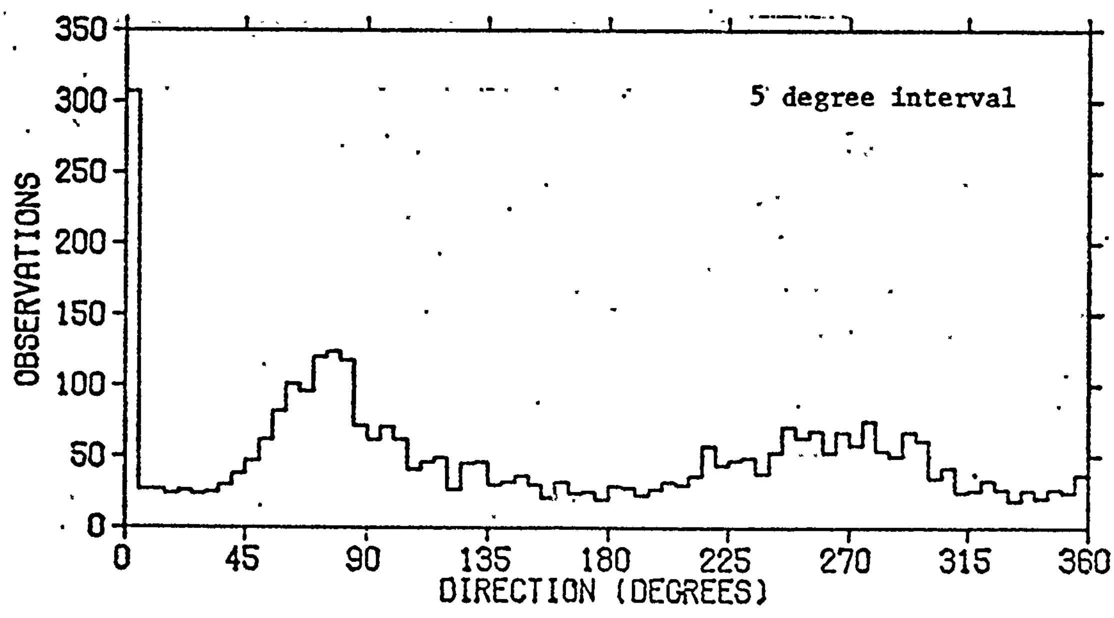

Figure 3. Current Direction Distribution (all data and all depths).

The sampling time-scale data of 56.25 seconds average was also examined for peak values during flood and ebb tide conditions. The summary of this analysis is shown in Table 4. As expected, the peak values slightly exceed the 15-minute averaged values of Table 3. To be noted is the frequent disparity between the ranges of peak current values for ebb and flood stages. For example, at 61-meter and 91-meter depth, the range of peak currents at ebb exceed those at flood. At 152-meter depth, the opposite condition occurs wherein the range of peak flood currents are significantly greater at flood than at ebb. At 274 meters, the ranges of peak currents are essentially equal for both flood and ebb.

The exhibited and presumed tidal current characteristics at various depths are summarized in Table 5. Histograms for current speed and direction (sample time = 56.25 sec) for 3.8 days duration at 30.5 meters are shown in Figures 4 and 5 respectively.

When PMEL priorities and funding provided by NTS allow, additional computer generated plots for speed and direction will be made for the remaining constant depth data.

5. Conclusions

a. The general current profile at Nanoose is complex both in speed fluctuation and direction.

b. Insufficient data were collected in this initial measurement to perform a harmonic analysis and thus correlate tidal currents with tidal variation (requires 29 days minimally to assess the influence of all the low frequency tidal constituents).

c. The peak currents measured at 274.3 meters (900 feet) are minimal compared to those at other depths. More important, however, is the indication the peak tidal current sets are 269° to 273° on flood and 81° to 96° on ebb. In other words, the major component of current is parallel to range centerline. The cross range currents are indicated as minimal.

d. Another long term current measurement (29 days) should be accomplished at 900-foot depth to increase the confidence in the above observation.

e. Depths shallower than 213.4 meters (700 feet) should not be utilized in ballistic measurements at Nanoose to preclude cross range current effects.

6. List of References

1. Woodward, William E. and Appel, Gerald F., *Report on the Evaluation of a Vector Averaging Current Meter*, NOAA-TM-NOS-NOIC-1, July 1973

2. Kalvaitis, A. N., *Effects of Vertical Motion on Vector Averaging (Savonius Rotor) and Electromagnetic Type Current Meters*, NOAA-TM-NOS-NOIC-3, March 1974

3. Vector Averaging Current Meter, Model 610, AMF Electrical Products Development Division, September 1973

TABLE 4. RANGE OF PEAK CURRENT STRENGTH AND DIRECTION

Nominal Depth Meters	Tide		Current cm/sec.		Direction-Degrees, Relative to +Y Range Axis	
	Flood	Ebb	Data Span	Mean	Data Span	Mean
61.0	---	X	14.0 to 21.7	15.8	67 to 80	74
91.4	X		8.2 to 13.4	10.8	128 to 292	246
		X	9.8 to 29.9	16.8	41 to 104	68
121.9	X		9.1 to 21.4	14.3	244 to 296	263
		X	*	3.3	*	74
152.4	X		25.9 to 39.8	30.4	281 to 298	291
		X	7.1 to 12.1	9.1	315 to 348	328
182.9 to 213.4	X		13.8 to 22.7	18.1	252 to 287	269
		X	*	5.6	*	254
274.3	X		7.1 to 13.6	10.35	269 to 273	271
		X	7.6 to 13.8	10.1	81 to 96	92
365.8	X	---	9.2 to 16.4	12.6	206 to 249	234

*Only 1 data point

TABLE 5. INDICATED PEAK TIDAL CURRENT CHARACTERISTICS

@ 30.5 meters: (100 ft)	There is no apparent preferred ebb or flood current set. The ebb current is stronger than the flodd current.
@ 61 meters: (200 ft)	The observed peak ebb current set ranges between 67° and 80°. The ebb current is stronger than the flood current.
@ 91.4 meters: (300 ft)	The observed peak current sets are delineated at ebb and flood stage in the 41° to 104° and 128° to 292° sectors respectively. Ebb strength generally exceeds the flood strength.
@152.4 meters: (500 ft)	The observed current set shifts from 281° to 298° at flood to 315° to 348° at ebb. The flood current strength is significantly greater than the ebb strength.
@183.9 to 213.4 meters: (600 to 700 ft)	Flood current sets ranged between 252° to 287°. Peak flood currents are stronger than ebb currents.
@274.3 meters: (900 ft)	The low flood and ebb currents strengths are comparable (∿14 cm/sec). Peak flood current sets ranged between 269° to 273°. Peak ebb current sets ranged between 81° to 96°.

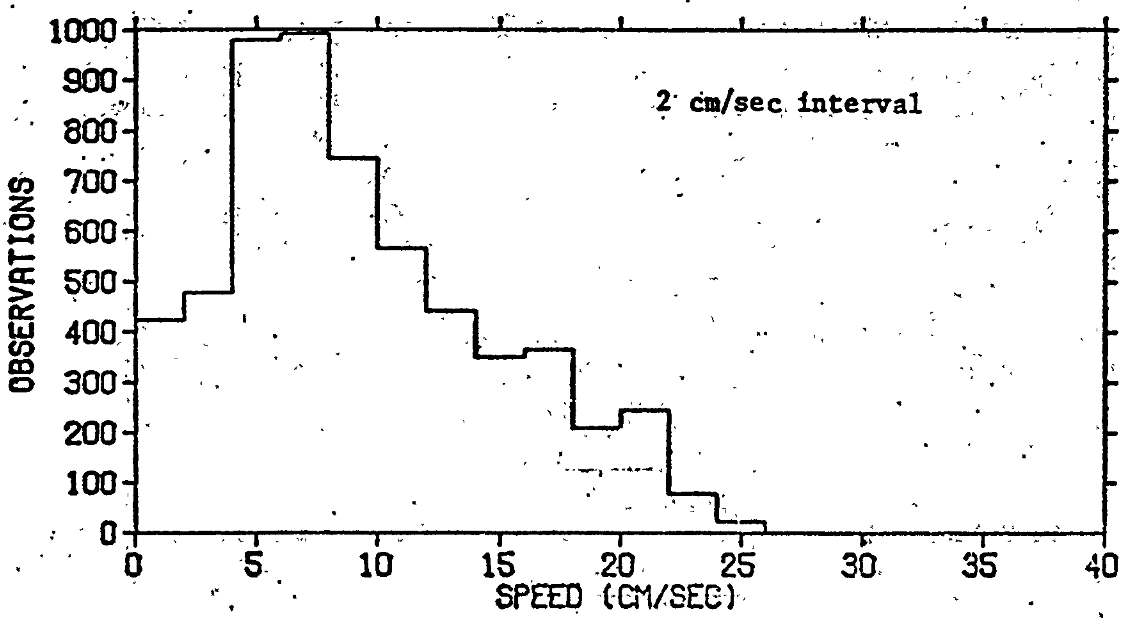

Figure 4. Current Speed Distribution at 30.5 meters

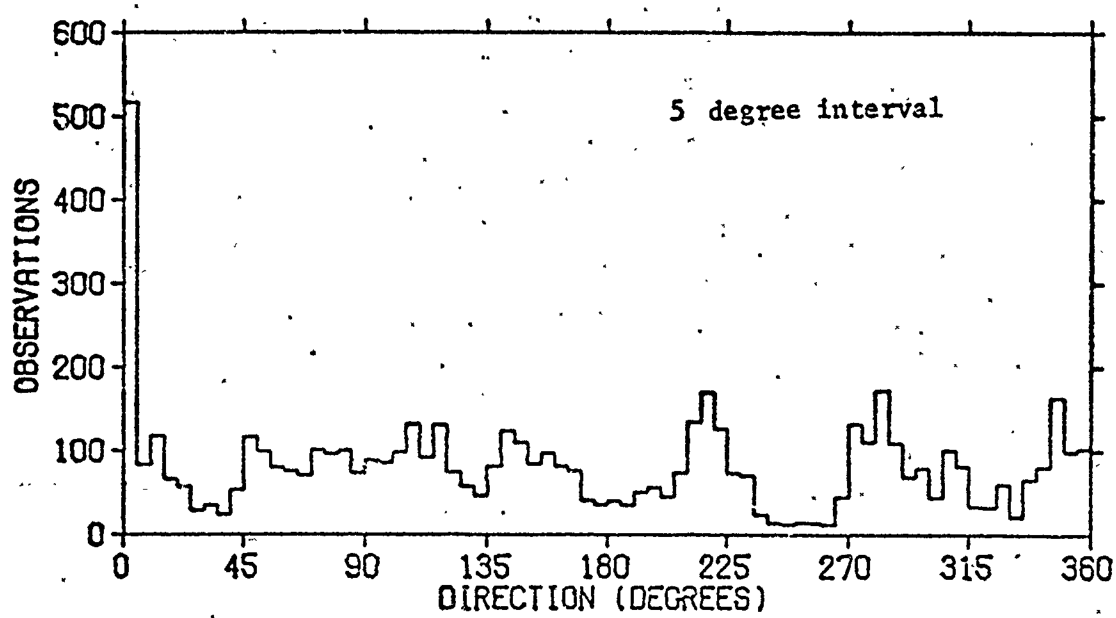

Figure 5. Current Direction Distribution at 30.5 meters.

Appendix B

RUN PLAN (RP) 9160

RUN PLAN 9160

TITLE BOMIS/VACM TEST

RANGE NANOOSE

CONTENTS	PAGE
1. TEST OBJECTIVES AND REQUIREMENTS	2
2. OPERATIONAL PROCEDURE	3,4
3. SAFETY INSTRUCTIONS	
4. SPECIAL INSTRUCTIONS	5,6
5. ABORT PROCEDURE	
6. INSTRUMENTATION	
OCEANOGRAPHIC MEASUREMENT & 3-D INSTRUMENTATION	7
OPTICAL MEASUREMENT	
RADAR REQUIREMENTS	
NOISE MEASUREMENTS	
TARGET SIMULATOR	
INTERROGATOR SYSTEM (MATIMS)	
WSAT SONAR CODES	
7. TEST VEHICLES PRESETS	
TORPEDO MK MOD	
TARGET MK MOD	
MOBILE TARGET MK 30 MOD 1 DATA FRAME SHEETS	
8. LAUNCHING CRAFT INSTRUCTIONS	
WIRE COMMANDS	
9. RECOVERY PROCEDURE	
10. TEST GEOMETRY	
DASH NUMBERS	
RUN GEOMETRY	

11. REVIEWERS *[illegible], HELTON*

PROJECT ENGINEER	CONTRACTOR	RUN MASTER
R. G. Welley		

BRANCH HD/DIVISION HD	TECH OPS
R. C. Peterson 3/4/76	*[illegible signature]*

SECURITY STATEMENT
UNCLASSIFIED

Page 1 of 7

DISTRIBUTION LIST

STANDARD	SPECIAL
511 (1)	7021 (2)
5121 (1)	7023 (3)
5041 (3)	811 (3) VIA 83 (NANOOSE ONLY)
52 (1)	7032 (1)
53 (1)	7041 (1)
70 (1)	
701 (1)	
8101H ~~(4) DABOB~~ (1) NANOOSE	
83 (5)	
837 (2)	
4011 (1)	

NTS 8510/500 (8/75)

UNCLASSIFIED

RUN PLAN 9160

1. **OBJECTIVES:** RECORD WATER CURRENTS AT 274 METERS DEPTH IN NANOOSE RANGE FOR ONE COMPLETE LUNAR CYCLE COMMENCING ON OR ABOUT 14 MAY 1976.

   a. INSTALL VECTOR AVERAGING CURRENT METER (VACM) ON BOMIS I.

   b. DEPLOY AT 900-FOOT DEPTH FOR 30 DAYS WITHOUT INTERRUPTION.

   c. NOTIFY HELTON OR WILLEY, EXT. 4261 IF DEPTH MUST BE CHANGED.

   d. REMOVE VACM AFTER COMPLETING THE TEST.

2. **OPERATING CRAFT:**

   A. LAUNCHING SHIPS

   B. TARGET BOATS

   C. SOUND BOATS

   D. RETRIEVER WITH DIVERS TO INSTALL AND REMOVE VACM

   E. GUARD BOATS

   F. AIR CRAFT

3. **INSTRUMENTATION:**

   A. 3-D DURING INSTALLATION AND REMOVAL

   B. SOUND RECORDING/NOISE MEASUREMENT

   C. OPTICAL

   D. TARGET

   E. FIRE CONTROL

   F. PRESSURE-VELOCITY

   G. OTHER VACM PROVIDED BY PMEL

4. **TORPEDOES:** (VACM:)

   A. ORDNANCE LOCATOR: 45 KHZ X 9 KHZ ____ SPECIAL ____

5. **COMMUNICATIONS:** MOTOROLA

6. **REFERENCES** R&E MEMO 62-76

PROJECT ENGINEER	DATE	TEST OBJECTIVES & REQUIREMENTS
K.G. Willey	4 Mar 76	PAGE 2 OF 7

UNCLASSIFIED

RUN PLAN 9160

STEP	INSTALLATION PROCEDURE	* ACTION
1	COORDINATE INSTALLATION PROCEDURE	OIC
2	RAISE BOMIS TO 10 FEET DEPTH	COMP
3	ASSEMBLE VACM, TANK, ROPES, SLEEVES, SHACKLES	TRB
4	UNDERWAY TOWARD BOMIS POSITION	TRB
5	TRACK BOMIS AND TRB	COMP
6	RECORD TWO ROTOR SPINS FOR TEMPORAL CORRELATION:	
	SPIN 4 MIN @ 000° VANE/RECORD START & STOP	702/COMP
	STOP 4 MINUTES	702
	SPIN 4 MINUTES @ 180° VANE/RECORD START & STOP	702/COMP
	STOP 4 MINUTES	702
7	CLOSE ON BOMIS POSITION	TRB
8	ALL STOP NEAR BOMIS. AVOID HULL CONTACT.	TRB
9	SECURE SAFETY LINE TO TANK	TRB
10	DIVERS ENTER WATER	DIVERS
11	DEPLOY VACM ASSEMBLY	TRB
12	ADJUST BOMIS DEPTH	COMP
13	SHACKLE VACM TO BOMIS	DIVERS
14	INSPECT VACM VANE AND ROTOR OPERATION	DIVERS
15	REPORT VACM OPERATIONAL	DIVERS/TRB
16	DETACH SAFETY LINE AND COME ABOARD	DIVERS
17	UNDERWAY FROM BOMIS AREA	TRB
18	LOWER BOMIS TO 900-FOOT DEPTH	COMP
19	LOG DEPTH SETTING AND TIME	COMP
20	END INSTALLATION PROCEDURE	ALL

*Target, Launcher, Computer, Noise Measuring, Retriever, Etc.

PROJECT ENGINEER	DATE	OPERATIONAL PROCEDURE
K. G. Willey	4 Mar 1976	PAGE 3 OF 7

NTS 8510/500-2 (1/75)

UNCLASSIFIED

UNCLASSIFIED

RUN PLAN 9160

STEP	REMOVAL PROCEDURE	* ACTION
1	COORDINATE REMOVAL PROCEDURE	OIC
2	TRACK BOMIS AND TRB	COMP
3	RAISE BOMIS TO 10 FOOT DEPTH	COMP
4	UNDERWAY TOWARD BOMIS POSITION	TRB
5	CLOSE ON BOMIS POSITION	TRB
6	ALL STOP NEAR BOMIS. AVOID HULL CONTACT	TRB
7	DIVERS ENTER WATER WITH SAFETY LINE	DIVERS
8	ADJUST BOMIS DEPTH	COMP
9	SECURE SAFETY LINE TO TANK	DIVERS
10	REMOVE VACM FROM BOMIS	DIVERS
11	BRING VACM ASSEMBLY ABOARD	TRB
12	DIVERS COME ABOARD	DIVERS
13	LOWER BOMIS TO OPERATIONAL DEPTH	COMP
14	RECORD TWO ROTOR SPINS FOR TEMPORAL CORRELATION:	
	SPIN 4 MIN @ 000° VANE/RECORD START AND STOP	702/COMP
	STOP 4 MIN	702
	SPIN 4 MIN @ 180° VANE/RECORD START AND STOP	702/COMP
	STOP 4 MIN	702
15	UNDERWAY FROM BOMIS AREA	TRB
16	END REMOVAL PROCEDURE	ALL

*Target, Launcher, Computer, Noise Measuring, Retriever, Etc.

PROJECT ENGINEER	DATE	OPERATIONAL PROCEDURE
K. G. Willey	4 Mar 76	PAGE 4 OF 7

UNCLASSIFIED

RUN PLAN 9160

STEP	INSTRUCTION
1	RANGE USERS HAVE BEEN CONTACTED AND THERE ARE NO FORESEEN REQUIREMENTS FOR BOMIS/VACM DEPTH EXCURSIONS DURING THE 30-DAY DEPLOYMENT PERIOD.
	a. BOMIS/VACM SHOULD REMAIN AT 900 FOOT DEPTH WITHOUT INTERRUPTION FOR THE ENTIRE 30 DAYS.
	b. SOUND SPEED AND 3-D TRACKING DATA WILL NOT BE REQUIRED DURING THE DEPLOYMENT PERIOD.
2	IF AN EMERGENCY DEVELOPS AND BOMIS/VACM DEPTH MUST BE CHANGED, PROCEED AS FOLLOWS:
	a. NOTIFY HELTON OR WILLEY, EXT. 4261, 2, or 4 PRIOR TO MOVING BOMIS/VACM IF TIME PERMITS.
	b. RECORD DATE, TIME AND DEPTH INFORMATION FOR EACH BOMIS/VACM DEPTH EXERCUSION.
	c. RETURN BOMIS/VACM TO 900 FOOT DEPTH AS SOON AS POSSIBLE AND RECORD TIME AND DATE OF TEST RESUMPTION.

PROJECT ENGINEER	DATE	
K. G. Willey	4 MAR 76	SPECIAL INSTRUCTIONS PAGE 5 OF 7

NTS 8510/500-4 (1/75)

UNCLASSIFIED

UNCLASSIFIED

RUN PLAN 9160

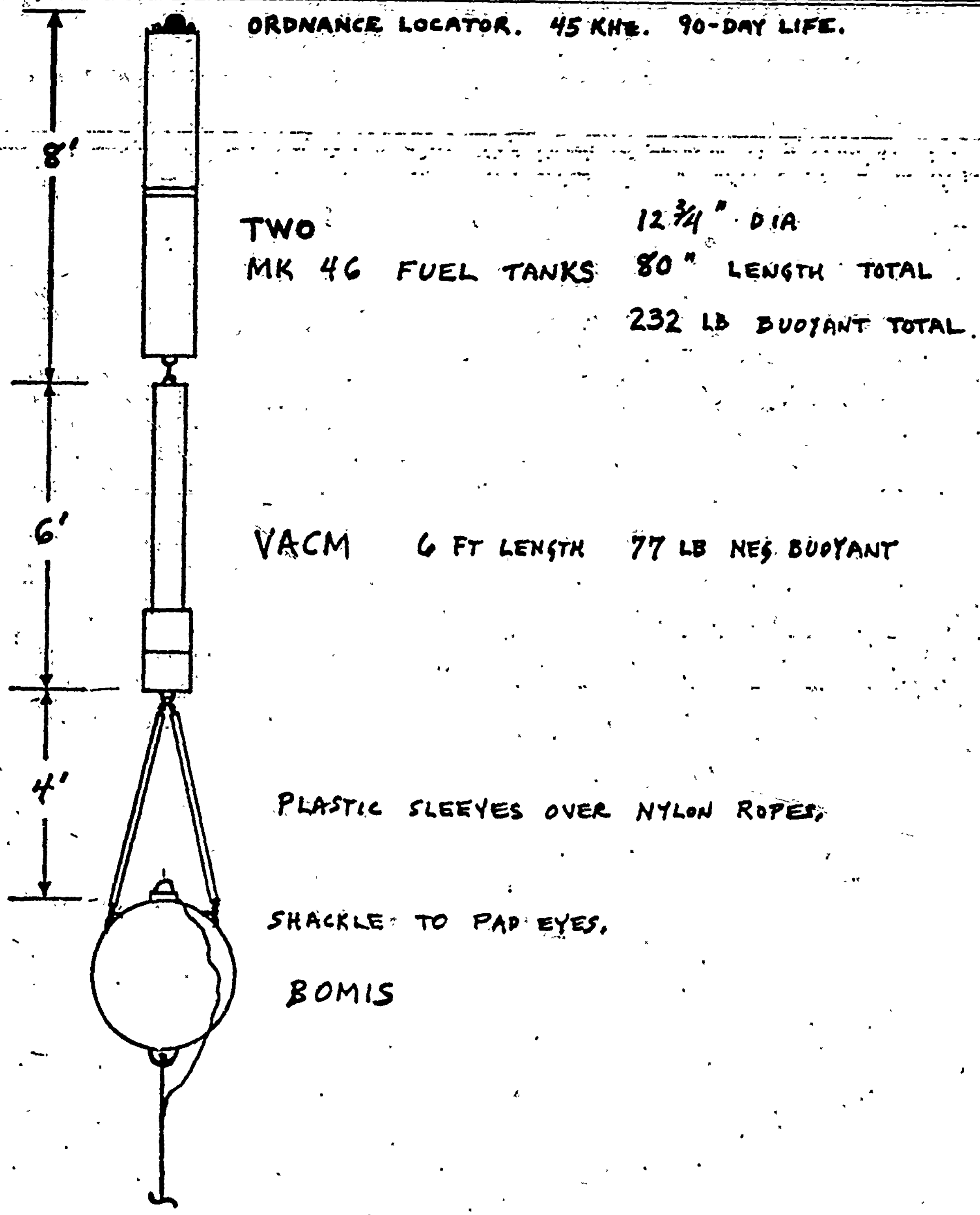

CONFIGURATION

PROJECT ENGINEER	DATE	SPECIAL INSTRUCTIONS
K. G. Willey	4 Mar 76	PAGE 6 OF 7

UNCLASSIFIED

UNCLASSIFIED

RUN PLAN 9160

THE VECTOR AVERAGING CURRENT METER

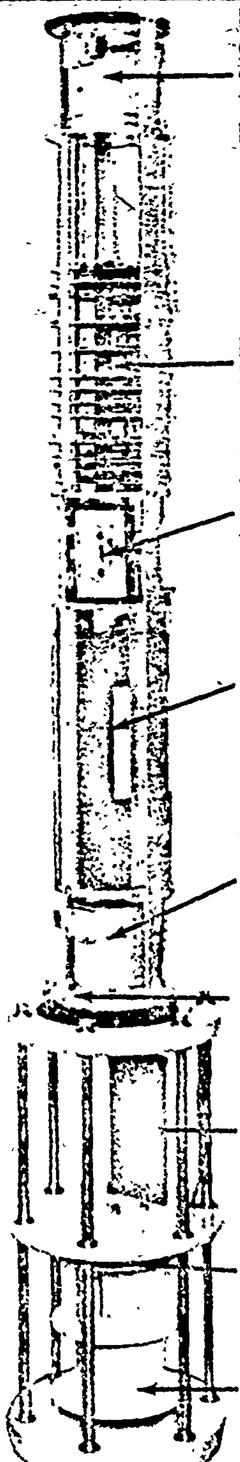

- Samples current speed and direction continuously every 1/8 turn of its rotor, in a 1-knot current, that's more than 660 samples per minute.
- Unique method of data computation allows computing, storing and recording actual Cartesian coordinate vector averages.
- Averages east and north current components over preset record period (15 minutes nominal).
- Averages temperature over same record period.
- Records digital data on a 4-track cassette magnetic tape recorder.
- Operates to 6,000-meter depths.
- Has a through-housing load capacity of 10,000 lbs.

SPECIFICATIONS:

Cassette Magnetic Tape Recorder: Records 3200 bits/inch at 400 bits/second, 11.5 x 10^6 bits total capacity
Sampling Rate: 8 per rotor turn
Current Speed: .05 to 6 knots
Current Direction: Compass 0° to 360°, vane 0° to 360°
Compass and Vane Direction Resolution: 2.8°
Operating Temperature Range: −2°C to 70°C
Thermistor Accuracy: ±0.10°C standard, ±0.01°C special
Timing Accuracy: ±10 ppm/day (i.e.: ±6 minutes/year)
Battery Life at Average 3-Knot Current Speed: Alkaline 6 months, mercury 1 year
Tensile Load Capacity: 10,000 lbs. through pressure housing
Weight: 160 lbs. in air. 77 lbs. in water
Outside Diameter: 10 15/16 in. rotor-vane cage, 7 1/2 in. pressure housing
Length: 77 1/2 in.
Top Eye Bolt: 1 1/2 in. I.D.
Bottom U Bolt: 2 in. I.D.

PROJECT ENGINEER	DATE	OCEANOGRAPHIC MEASUREMENT VACM
K. G. Willey	4 Mar 76	PAGE 7 OF 7

Appendix C

SUB-PERIOD CURRENT SPEED AND DIRECTION CHARACTERISTICS

RANGE COORDINATE SYSTEM
OBSERVATION PERIOD = 2330 18 MAY 76 TO 2300 25 MAY 76 (7.0 DAYS)
N = 336, DT = 30.00 MINUTES, UNITS = (CM/SEC) (TIMES ARE GMT)

	MEAN	VARIANCE	ST-DEV	SKEW	KURT	MAX	MIN
S	5.64	8.45	2.91	.139	3.200	15.79	.00
U	-.02	25.65	5.06	.096	2.272	14.24	-9.89
V	2.49	8.41	2.90	-.753	3.876	8.39	-6.95

S = SPEED
U = ALONG-RANGE COMPONENT OF VELOCITY, 103°TN = POSITIVE U
V = CROSS-RANGE COMPONENT OF VELOCITY, 13°TN = POSITIVE V

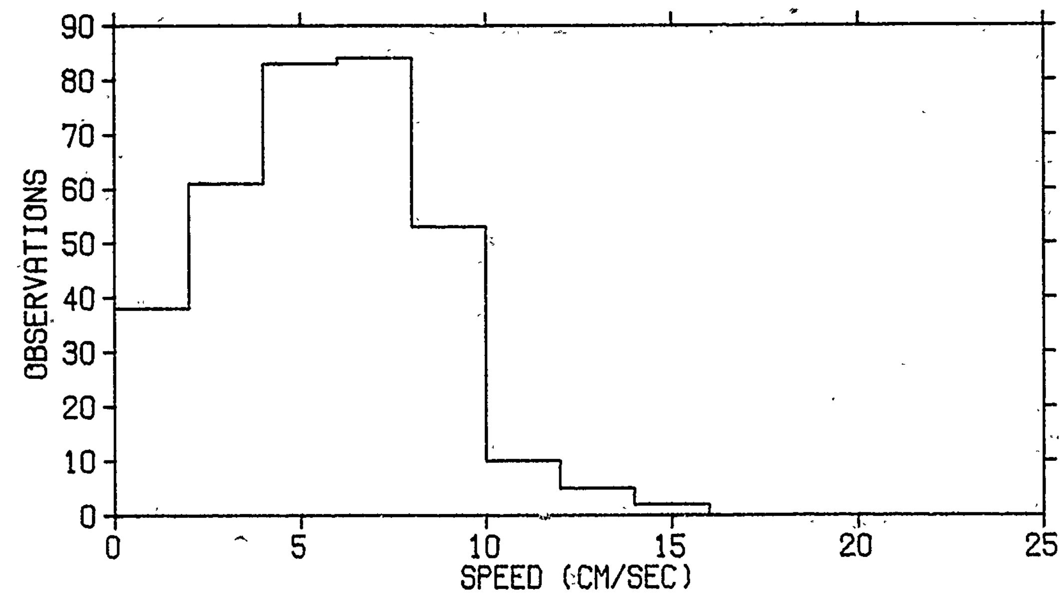

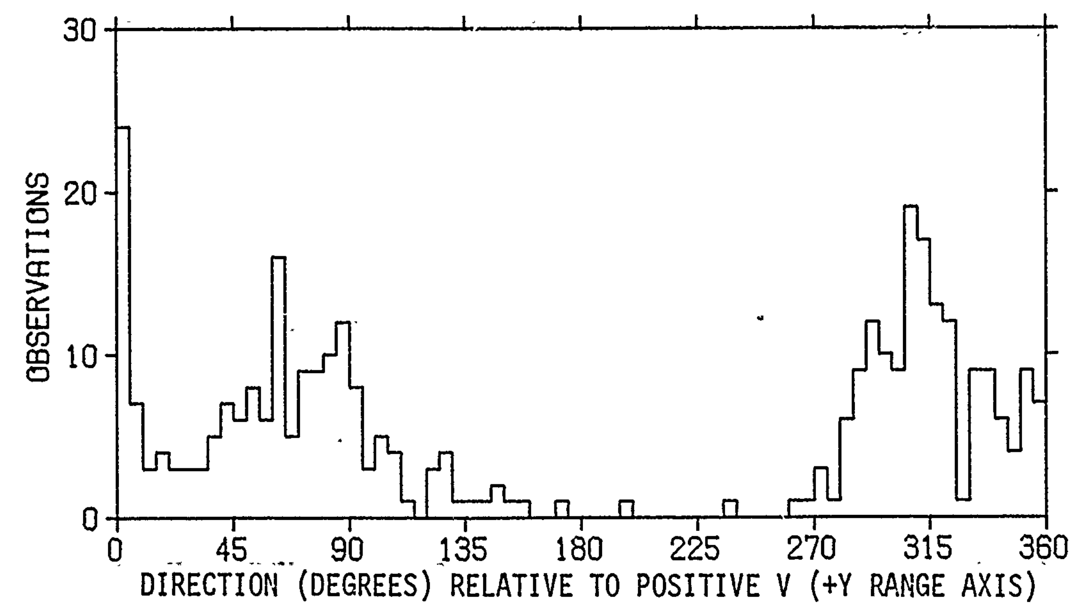

Figure C-1. Statistics and Histograms of Currents at BOMIS, 1976
18 May to 25 May 1976

RANGE COORDINATE SYSTEM
OBSERVATION PERIOD = 2330 25 MAY 76 TO 2300 1 JUN 76 (7.0 DAYS)
N = 336, DT = 30.00 MINUTES, UNITS = (CM/SEC) (TIMES ARE GMT)

	MEAN	VARIANCE	ST-DEV	SKEW	KURT	MAX	MIN
S	6.35	13.69	3.70	.473	2.659	16.74	.00
U	-1.00	46.39	6.81	-.126	2.184	12.98	-15.97
V	.35	6.53	2.55	-.013	2.551	6.32	-5.85

S = SPEED
U = ALONG-RANGE COMPONENT OF VELOCITY, 103°TN = POSITIVE U
V = CROSS-RANGE COMPONENT OF VELOCITY, 13°TN = POSITIVE V

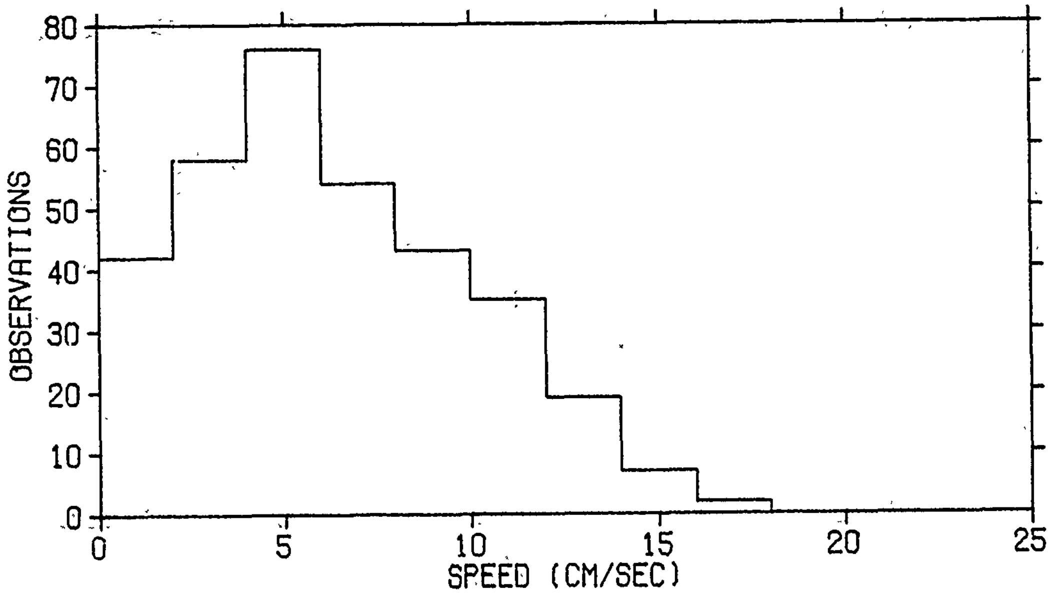

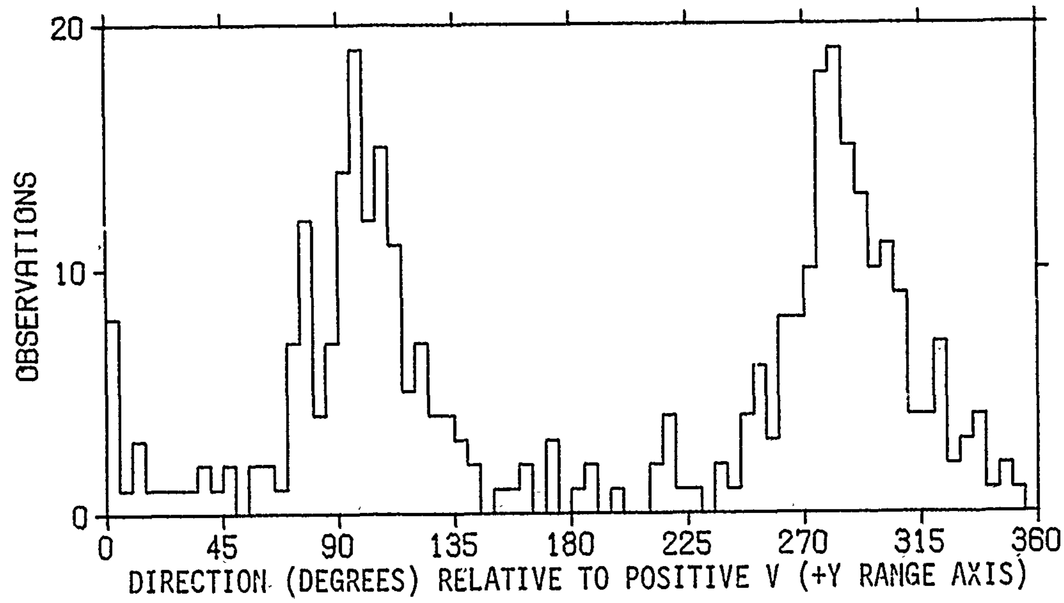

Figure C-2. Statistics and Histograms of Currents at BOMIS, 1976
25 May to 1 June 1976

RANGE COORDINATE SYSTEM
OBSERVATION PERIOD = 2330 1 JUN 76 TO 2300 8 JUN 76 (7.0 DAYS)
N = 336, DT = 30.00 MINUTES; UNITS = (CM/SEC) (TIMES ARE GMT)

	MEAN	VARIANCE	ST-DEV	SKEW	KURT	MAX	MIN
S	6.90	15.18	3.90	1.026	4.571	20.59	.00
U	-1.89	49.37	7.03	-.342	2.518	10.62	-20.04
V	.78	9.27	3.04	-.202	2.442	6.83	-8.27

S = SPEED
U = ALONG-RANGE COMPONENT OF VELOCITY, 103°TN = POSITIVE U
V = CROSS-RANGE COMPONENT OF VELOCITY, 13°TN = POSITIVE V

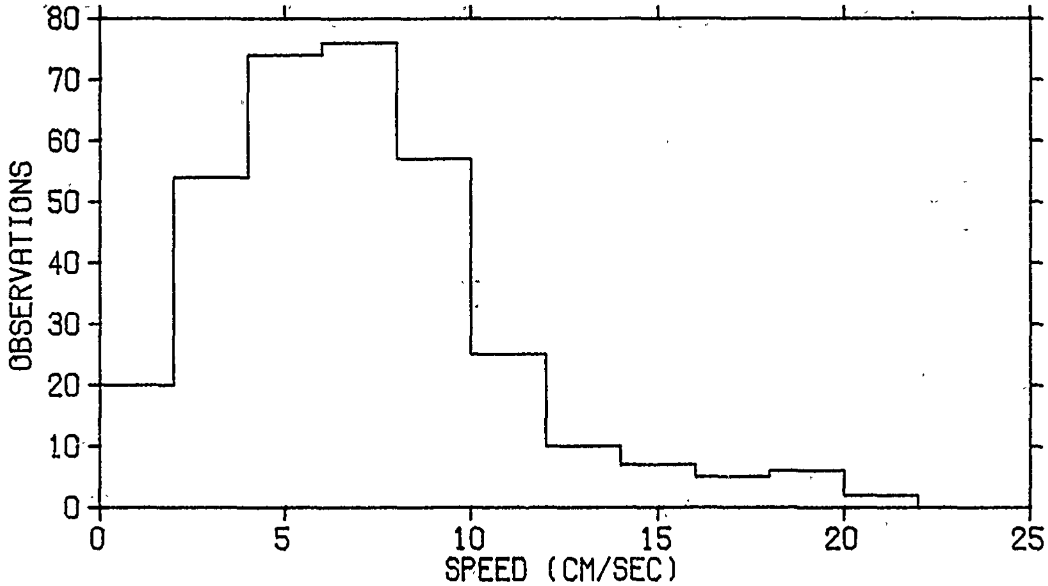

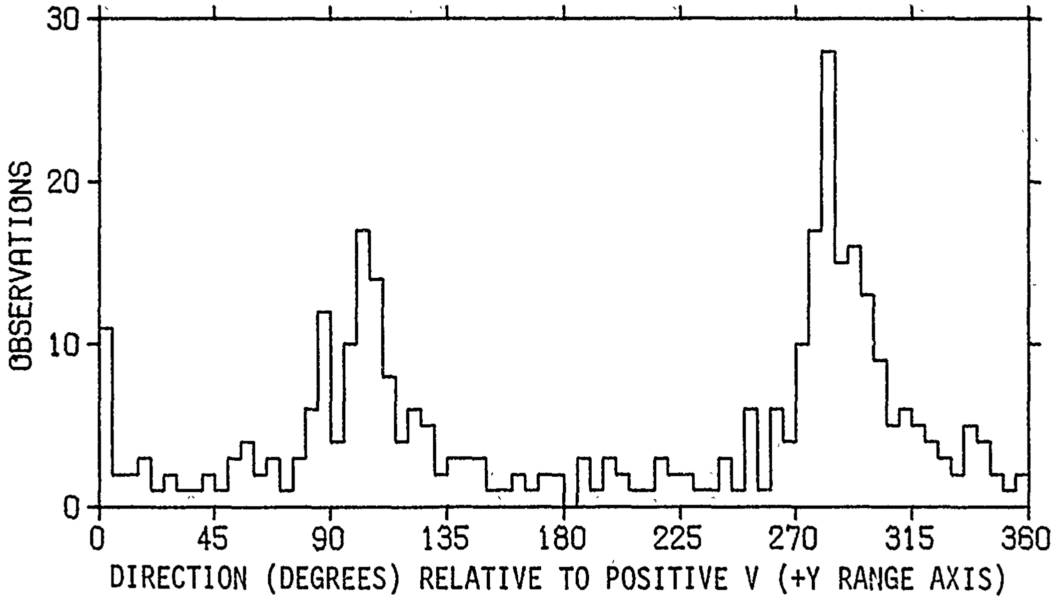

Figure C-3. Statistics and Histograms of Currents at BOMIS, 1976
1 June to 8 June 1976

RANGE COORDINATE SYSTEM
OBSERVATION PERIOD = 2300 8 JUN 76 TO 1430 18 JUN 76 (9.7 DAYS)
N = 464, DT = 30.00 MINUTES, UNITS = (CM/SEC) (TIMES ARE GMT)

	MEAN	VARIANCE	ST-DEV	SKEW	KURT	MAX	MIN
S	8.18	17.94	4.24	.453	2.562	20.30	.00
U	-.58	72.73	8.53	-.020	2.134	18.96	-19.24
V	-.47	11.51	3.39	.133	2.255	7.15	-8.34

S = SPEED
U = ALONG-RANGE COMPONENT OF VELOCITY, 103°TN = POSITIVE U
V = CROSS-RANGE COMPONENT OF VELOCITY, 13°TN = POSITIVE V

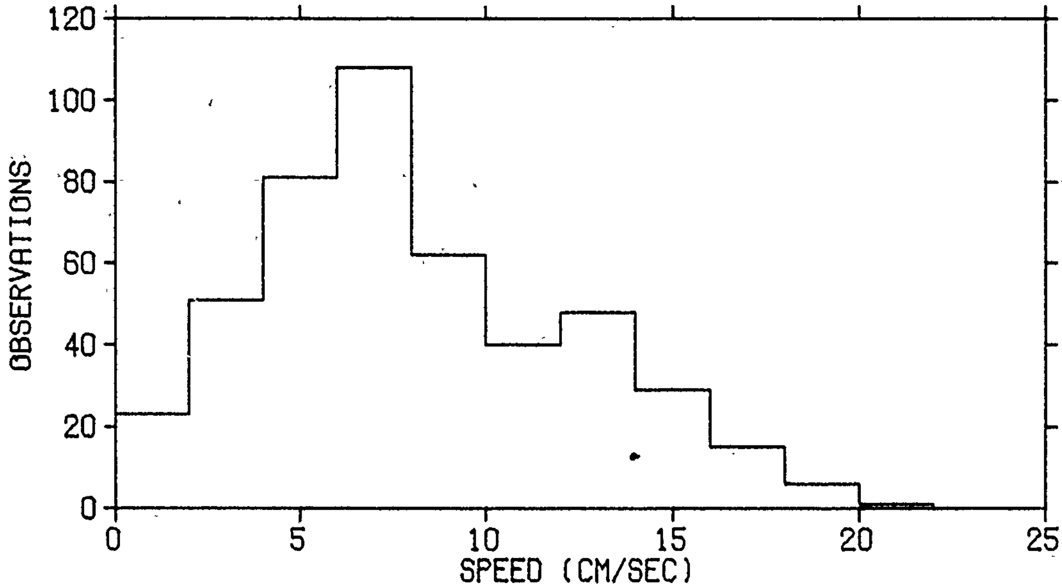

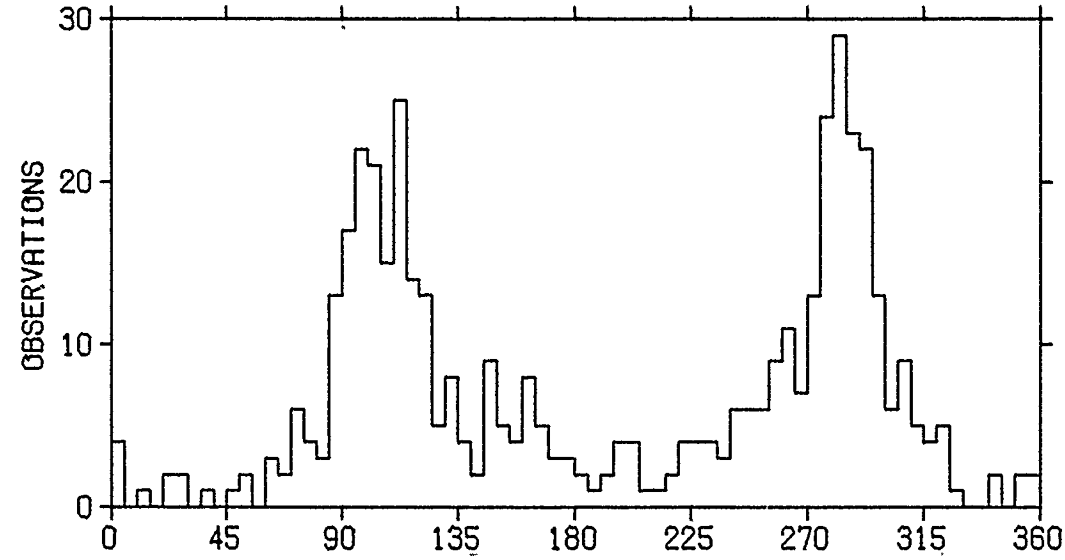

Figure C-4. Statistics and Histograms of Currents at BOMIS, 1976
8 June to 18 June 1976

Appendix D

INSTRUCTIONS FOR CURRENT PREDICTION

1. Node factors N_i and equilibrium arguments $(V_o+U)_i$ are entered into the program for each specific year and tidal component. Figure D-1 is the HP 9820 current prediction program for Station 32 with the factors for CY 1976. These data for other years are provided in Tables 11 and 13.

2. Prediction time (hours into year commencing at 0000 1 January) are entered as desired. Figure D-1 shows the prediction time from 3328 hours to 4062 hours.

3. After entering program and END RUN PROGRAM the plot variable is requested

a. RUN PROGRAM: plots cross-range current prediction
b. Enter 20 RUN PROGRAM: plots along-range current prediction
c. Enter 19 RUN PROGRAM: plots current speed prediction

PREDICTIVE
TIME SPAN

```
0:
21→Z;DSP "PLOT V
ARIABLE?";STP ⊢
1:
Z→B⊢
2:
SCL 3328,4062,-2
5,25⊢
3:
AXE 3328,0,24,5⊢
4:
3328→A⊢
5:
.916*3.8687*COS
(15.041068*A+16.
2-101.23)→R1⊢
6:
.863*1.7297COS (
13.943035*A+6.5-
71.24)→R2⊢
7:
1*1.2417*COS (14
.95893*A+350.2-1
01.23)→R3⊢
8:
1.029*4.0108*
COS (28.98410*A+
26.0-76.61)→R4⊢
9:
1*1.1593*COS (30
.0*A+0.0-134.38)
→R5⊢
10:
.804*.3156*COS (
30.08214*A+211.5
-134.38)→R6⊢
11:
1.029*.8221*COS
(28.43973*A+305.
3-53.61)→R7⊢
12:
1.059*.5941*COS
(57.96821*A+52.1
0-102.07)→R7⊢
13:
R1+R2+R3+R4+R5+R
6+R7+R8→R9⊢
14:
.916*4.5338*COS
(15.041068*A+16.
2-275.34)→R10⊢
15:
.863*2.5961*COS
(13.943035*A+6.5
-258.56)→R11⊢
16:
1*1.4553*COS (14
.95893*A+350.2-2
75.34)→R12⊢
17:
1.029*3.7446*
COS (28.98410*A+
26.0-253.63)→R13
⊢
18:
1*1.6808*COS (30
.0*A+0.0-301.48)
→R14⊢
19:
.804*.4571COS (3
0.08214*A+211.5-
301.48)→R15⊢
20:
1.029*.7676*COS
(28.4397*A+305.3
-230.63)→R16⊢
21:
1.059*.6054*COS
(57.96821*A+52.1
0-299.54)→R17⊢
22:
R10+R11+R12+R13+
R14+R15+R16+R17+
R18⊢
23:
√(R9↑2+R18↑2)→R1
9⊢
24:
R18*COS 78-R9*
SIN 78→R20⊢
25:
-(R18*SIN 78+R9*
COS 78)→R21⊢
26:
PLT A,RB⊢
27:
A+1→A⊢
28:
IF A≤4062;GTO 5⊢
29:
END ⊢
R1319
```

Figure D-1. HP 9820 Current Prediction Program for Station 32

DISTRIBUTION

	Copy
NAVSEASYSCOM (PMS 402)	1
(PMS 405)	2
(PMS 406)	3
(SEA 06HB)	4
NUSC, Newport (D. Shonting)	5
NSWC, Silver Spring	6
NOSC, San Diego (H.A. Schenck)	7
(F. Marshall)	8
NSRDC, Washington, DC	9
NCSL, Panama City, FL	10
Naval Postgraduate School, Monterey, CA (D.A. Stentz)	11
(D.F. Leipper)	12
(J.V. Sanders)	13
APL/Johns Hopkins University (D. Wenstrand)	14
APL/University of Washington (G.R. Garrison)	15
(E.R. Linger)	16
(D. Haugen)	17
University of Washington, Department of Oceanography (E.E. Collias)	18
Pacific Marine Environmental Laboratory NOAA, Seattle (D. Halpern)	19
(J. Holbrook)	20
University of British Columbia (Dr. P.B. Crean)	21
A/Regional Tidal Superintendent Pacific Region, Marine Sciences Directorate, 512 Federal Building, Victoria, BC (W.J. Rapatz)	22
Maritime Experimental and Test Range, Nanaimo V9 R5 N3 (Keith Kitching)	23
DDC (TIMA) via form 50	24,25
NAVTORPSTA (Code 05G)	26
50	27
502	28
503	29
506	30
51	31
521	32
54	33
70	34
7002	35

--continued

DISTRIBUTION --concluded

		Copy
NAVTORPSTA (Code	702)	36
	7022 (Kelf)	37
	7023A	38
	7023H	39
	7032 (R.A. Daniel)	40
	704	41
	800	42
	8003	43
	801	44
	803 (CDR Moore)	45
	0115	46 through 50